CRREL REPORT 96-4

Geological and Geophysical Investigations of the Hydrogeology of Fort Wainwright, Alaska

Part I: Canol Road Area

Daniel E. Lawson, Jeffrey C. Strasser, Jodie D. Strasser,
Steven A. Arcone, Allan J. Delaney and Christopher Williams

May 1996

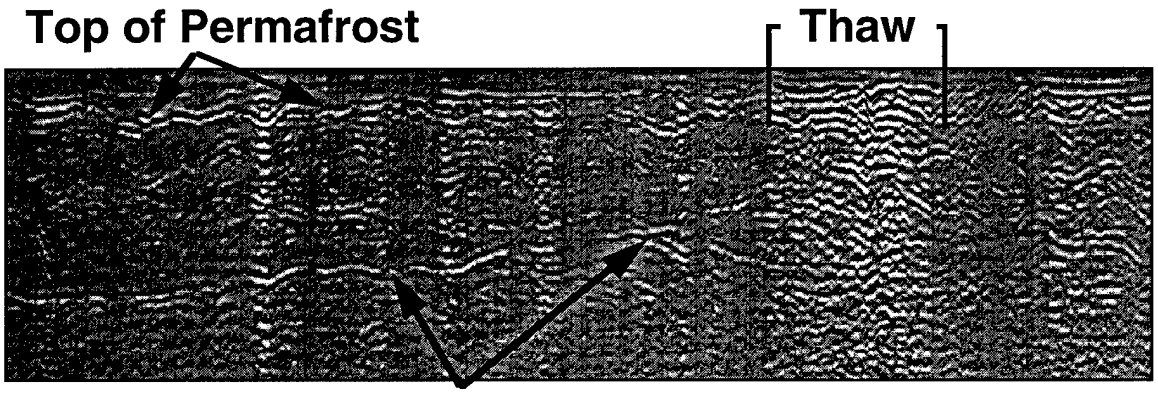

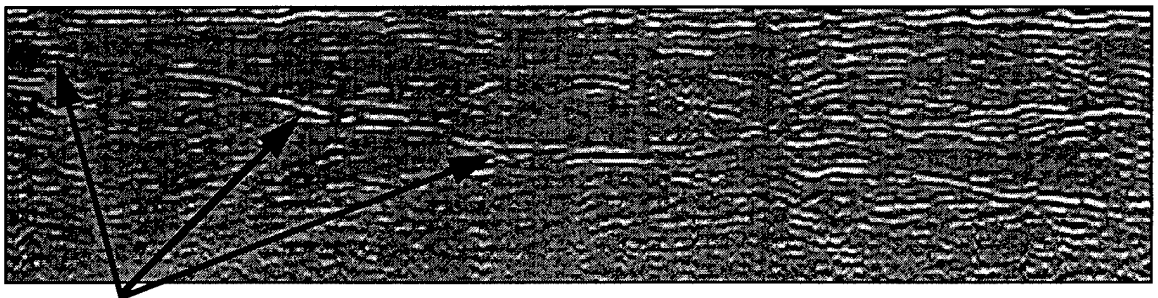

Abstract: The hydrogeology of Fort Wainwright, Alaska, is extremely complex because of the relatively impermeable discontinuity of permafrost, which controls the distribution and dimensions of the aquifer. Aquifers occur above, below and adjacent to permanently frozen materials, as well as within thaw zones surrounded by permafrost. This complexity makes it difficult to predict the direction and rate of ground water flow, as well as its seasonal and annual variability. Considerable problems exist in locating suspected contaminant plumes, identifying source areas, defining transport paths and evaluating contaminant fate. This report summarizes the results of ongoing investigations of the permafrost and ground water conditions within the northwestern part of the Fort Wainwright cantonment area, north of the Chena River. Data from ground-penetrating radar, drilling, ground water flow sensors, aerial photographs and ground observations were used to delineate aquifer distribution and develop a conceptual physical model of hydrogeological conditions. Ground water seepage velocity and direction, which were measured during early to mid-winter 1994–95, reflect the role of local water sources and permafrost distribution in determining ground water flow patterns. Other factors, including the vertical and lateral extent of permafrost, a bedrock aquifer, and the alluvial origins of unfrozen sediments and landforms, are apparently more important than the subregional aquifer in determining ground water conditions during winter. Contaminant migration will be strongly affected by these factors as well.

Cover: Two examples of ground-penetrating radar profiles of permafrost and ground water on Fort Wainwright, Alaska. The data are deconvolved 100-MHz profiles of transects G5 (top) and G7 acquired in September 1993. Distance is along the x-axis (280 m for G5 and 120 m for G7). The y-axis represents 500 ns for both transects. The profiles show a discontinuous response within the first 100 ns to the permafrost table, and a continuous response at approximately 100–400 ns to the subpermafrost water. Areas that have no permafrost are indicated.

How to get copies of CRREL technical publications:

Department of Defense personnel and contractors may order reports through the Defense Technical Information Center:

DTIC-BR SUITE 0944
8725 JOHN J KINGMAN RD
FT BELVOIR VA 22060-6218
Telephone 1 800 225 3842
E-mail help@dtic.mil
msorders@dtic.mil
WWW http://www.dtic.dla.mil/

All others may order reports through the National Technical Information Service:

NTIS
5285 PORT ROYAL RD
SPRINGFIELD VA 22161
Telephone 1 703 487 4650
1 703 487 4639 (TDD for the hearing-impaired)
E-mail orders@ntis.fedworld.gov
WWW http://www.fedworld.gov/ntis/ntishome.html

A complete list of all CRREL technical publications is available from:

USACRREL (CECRL-TL)
72 LYME RD
HANOVER NH 03755-1290
Telephone 1 603 646 4338
E-mail techpubs@crrel.usace.army.mil

For information on all aspects of the Cold Regions Research and Engineering Laboratory, visit our World Wide Web site: http://www.crrel.usace.army.mil

CRREL Report 96-4

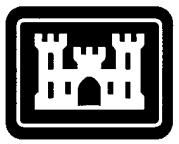

US Army Corps of Engineers
Cold Regions Research & Engineering Laboratory

Geological and Geophysical Investigations of the Hydrogeology of Fort Wainwright, Alaska

Part I: Canol Road Area

Daniel E. Lawson, Jeffrey C. Strasser, Jodie D. Strasser,
Steven A. Arcone, Allan J. Delaney and Christopher Williams

May 1996

Prepared for
U.S. ARMY ENGINEER DISTRICT, ALASKA

PREFACE

This report was prepared by Dr. Daniel E. Lawson, Research Physical Scientist, Jeffrey C. Strasser, Physical Scientist, Jodie D. Strasser, Physical Scientist, Geological Sciences Division, Dr. Steven A. Arcone, Geophysicist, Allan J. Delaney, Physical Science Technician, Snow and Ice Division, and Christopher Williams, Electronics Engineer, Engineering Resources Branch, U.S. Army Cold Regions Research and Engineering Laboratory.

The investigations described in this report were conducted through the U.S. Army Engineer District, Alaska, for the Environmental Resources Department, Public Works Directorate, U.S. Army, Alaska, under two projects: *Geological and Geophysical Analyses of Permafrost and Ground Water Conditions, Fort Wainwright, Alaska,* and *Site-specific, In Situ Ground Water Flow Analyses at Fort Wainwright, Alaska.* The authors thank Cristal Fosbrook, Chief, Environmental Restoration Branch, and Douglas Johnson, Chief, Environmental Resources Department, USARAK, Fort Richardson, Alaska, for their continued support, encouragement and assistance in many aspects of the work on Fort Wainwright.

The authors also thank the personnel in the Alaska District's Geotechnical Branch for obtaining and evaluating subsurface data by drilling the ground-truth boreholes that are an essential element in interpreting and applying the ground-penetrating radar transect data. In particular they thank Jerry Raychel, Chief, Soils and Geology, Del Thomas, Chief, Geotechnical Branch, and the many members of the District's field crews responsible for logging and sampling each hole, including James Sauceda, Chuck Wilson, Joni Sue Minor and Jeff Hitch. The Alaska District's drill crew, and the contracted drill crew for Ambler, Inc., particularly driller Dan Finnegan, are to be commended for drilling and obtaining borehole information even under the most trying of field conditions and weather.

CONTENTS

ILLUSTRATIONS

Figure

TABLE

Geological and Geophysical Investigations of the Hydrogeology of Fort Wainwright, Alaska

Part I: Canol Road Area

DANIEL E. LAWSON, JEFFREY C. STRASSER, JODIE D. STRASSER,
STEVEN A. ARCONE, ALLAN J. DELANEY AND CHRISTOPHER WILLIAMS

INTRODUCTION

Within interior Alaska, and, in particular, the cantonment area of Fort Wainwright, the permanently frozen and unfrozen materials that contain ground water aquifers are complexly and discontinuously distributed. Ground water may occur above, below and adjacent to those materials, as well as in thawed zones that are within, or penetrate through, the permafrost. The permafrost controls the movement of ground water because of its impermeability.

The fate of contaminants in ground water is thereby linked to both the distribution of permafrost and the movement of the ground water within the adjacent unfrozen sediments. Prior to the work discussed in this report, permafrost and aquifer distributions across Fort Wainwright were incompletely described and known only in general terms. Therefore, the complex hydrogeological conditions led to considerable problems for those trying to locate suspected contaminants, to identify source areas, to define transport paths, and to evaluate the fate of contaminant plumes, including their migration off-site. Physical hydrogeological models of ground water flow in this permafrost terrain are therefore essential to remediating contamination.

Permafrost may be present or absent because of a number of factors, including human and natural disturbances to the terrain and vegetation, and its distribution may therefore be chaotic. Identifying areas of permafrost and, conversely, unfrozen aquifers within permafrost areas is therefore extremely difficult. Standard techniques such as drilling or terrain analyses cannot readily locate frozen or unfrozen zones except in the most obvious of cases.

In this report, we summarize the initial results of ongoing hydrogeological investigations of the ground water and permafrost conditions in the northwestern corner of the cantonment of Fort Wainwright. Our work has included developing Ground-Penetrating Radar (GPR) to define the spatial and vertical extent of permafrost. Our investigations are part of continuing site characterization for remedial investigations and treatability studies of contaminant problems on Fort Wainwright (Fig. 1). This facility was placed on the Comprehensive Environmental Response, Compensation, and Liability Act (CERCLA) National Priorities List (NPL) in August 1990. The Canol Road area contains two sites within one of the five Operable Units (OU-3) established for investigation and remediation under the Federal Facilities Agreement (FFA) of 1992, which sets guidelines for Fort Wainwright on contaminant remediation under CERCLA.

General background

The three-dimensional distribution of permanently frozen ground exerts considerable control on ground water flow in regions of discontinuous permafrost. Transitions from unfrozen to frozen conditions may be abrupt and without surface expression. Further complicating our attempts to define this distribution are several factors: the current environment, past climatic conditions, terrain characteristics, vegetation cover, historic use and surface disturbances (Hopkins et al. 1955, Williams 1970).

Permafrost exists at various depths throughout the Fairbanks and Fort Wainwright area. The top of the permafrost ranges from 0.5 to over 15 m deep, with the thickest thawed zones beneath

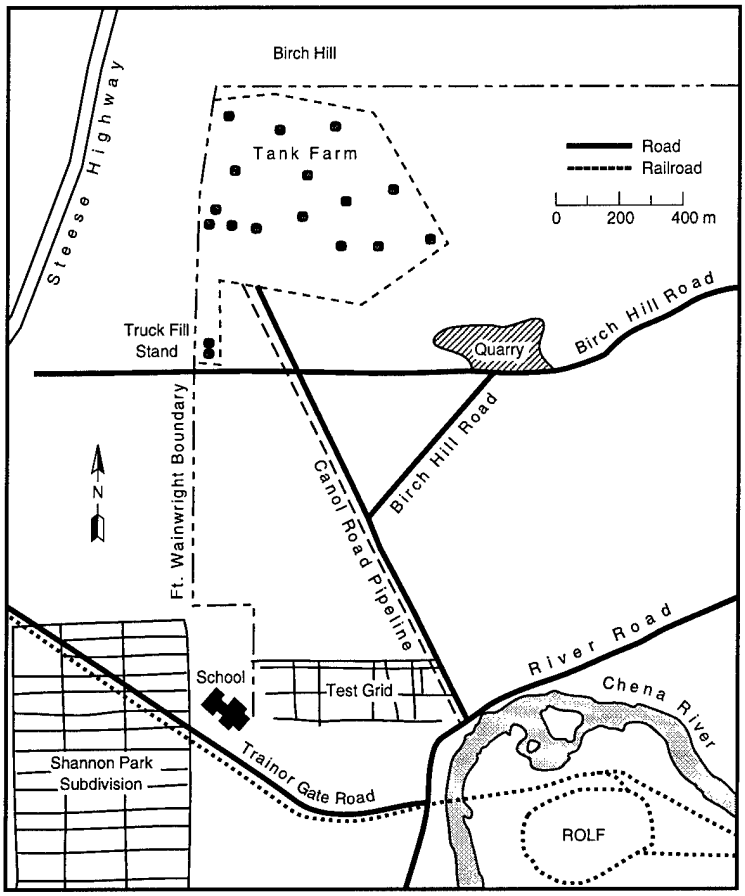

Figure 1. OU-3 sites north of the Chena River, including the Tank Farm, Truck Fill Stand, Canol Road pipeline and Test Grid.

swales or former stream channels, roads, buried pipelines, building excavations and other areas cleared of vegetation (Lawson et al. 1993). The bottom surface of the permafrost commonly ranges from 10 to over 50 m deep, with a minimum thickness of a few meters adjacent to thawed areas, and maximum thicknesses over 80 m in areas that may be some of the geologically oldest surficial materials on Fort Wainwright. The top and bottom surfaces of the permafrost also have highly irregular relief and can substantially influence ground water movement (Fig. 2).

Ground water flow within the cantonment area of Fort Wainwright (Fig. 1) is necessarily complex. This complexity reflects not only the presence or absence of permafrost but also the structure and stratigraphy of the surface sediments, the thickness of unfrozen materials above the permafrost, the total thickness and depth to the bottom of permafrost, and the immediate sources of ground water. These sources include the Chena–Tanana River system and more local aquifers such as Birch Hill (Péwé 1958, Williams 1970, Shannon and Wilson, Inc. 1992, Lawson et al. 1993).

Two types of ground water systems exist: a laterally discontinuous, near-surface system above the permafrost (suprapermafrost), and a deeper one beneath the permafrost (subpermafrost) (Lawson et al. 1993). The suprapermafrost and subpermafrost aquifers are linked where the frozen ground is perforated by isolated thaw zones (surrounded by permafrost, but unfrozen to bedrock), and in more extensive unfrozen zones, typically within former stream channel or swale deposits. Isolated thaw zones (taliks) may be areas where the subpermafrost aquifer discharges or recharges, exhibiting either upward or downward vertical

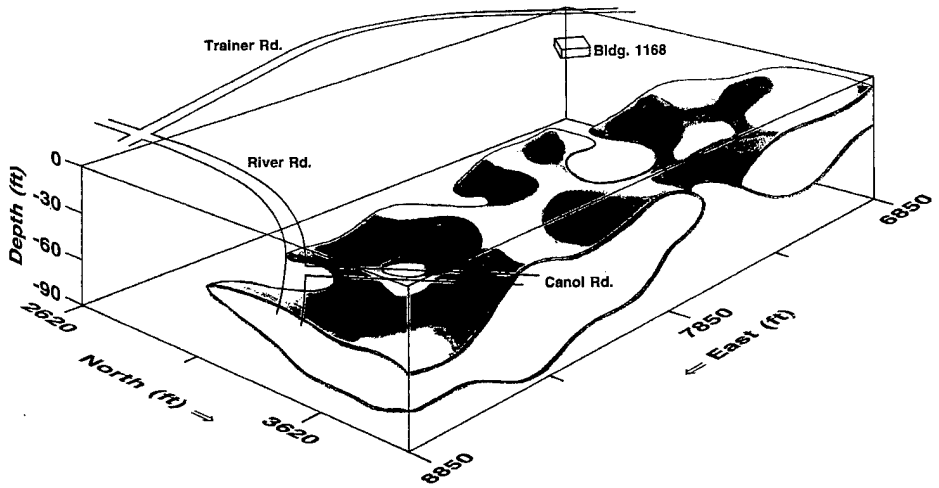

Figure 2. Stacked, three-dimensional representations of upper and lower surfaces of permafrost in the Canol Road "Test Grid." Permafrost is absent in those areas of the figure where the upper surface appears to be at a lower elevation than the bottom surface.

gradients. The near-surface systems may also be confined spatially by permafrost, with little or no connection to a subpermafrost aquifer. Water levels, flow rates and flow directions in such a perched aquifer may vary seasonally and diurnally in ways that are significantly different from the general trends in the regional aquifer. This may happen where the active layer or annual depth of thaw is shallow (less than 1.0 m). The subpermafrost aquifer can also be locally confined or isolated by areas of materials that are permanently frozen into the underlying bedrock.

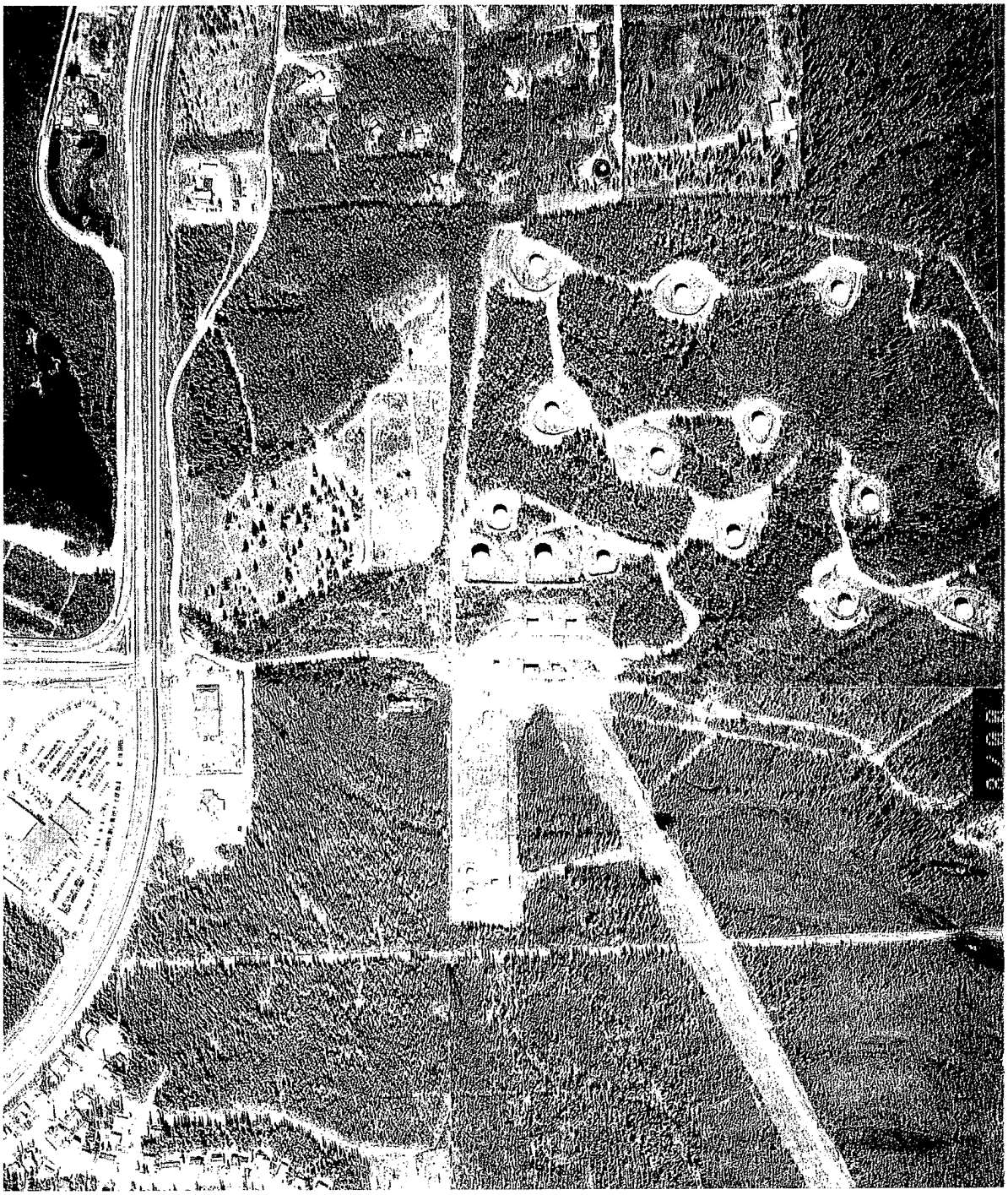

Figure 3. Aerial photograph of the discontinuous permafrost region generally north of the Chena River. Photo taken 20 May 1993.

Surficial and bedrock geology

Unconsolidated deposits of the Chena River and its smaller tributaries make up most of the surficial materials south of Birch Hill (Péwé et al. 1976). These deposits are mainly former point bars, swales, channels or sloughs, and related overbank deposits resulting from alluvial processes. Drilling has revealed that most of the surficial deposits on Fort Wainwright consist of gravels and sands, with sporadic silt layers and lenses (U.S. Army Engineer District, Alaska, unpublished borehole records). There is a layer of silt, usually less than 1 m thick, typically just below a surface layer of organics.

The unconsolidated materials of the Chena River floodplain lie unconformably above dark pelitic schists of the Yukon–Tanana Complex (King 1969), formerly identified as the Birch Creek Schist (Péwé et al. 1976). This metamorphic unit is generally of lower greenschist facies, and the age, although controversial, is thought to be pre-Jurassic (Péwé et al. 1976). Birch Hill, which bounds the northern part of the cantonment, is also composed of this highly fractured and foliated schist. In most areas of Birch Hill, the bedrock is overlain by eolian silt with thicknesses that may exceed 3 m or more. Various processes have moved weathered bedrock and silt downslope off Birch Hill, forming heterogeneous deposits of mixed grain sizes, colluvium, peripheral to its base.

Site descriptions

The OU-3 sites that are under investigation in the Canol Road area include the Tank Farm, the Truck Fill Stand and the Canol Road pipeline

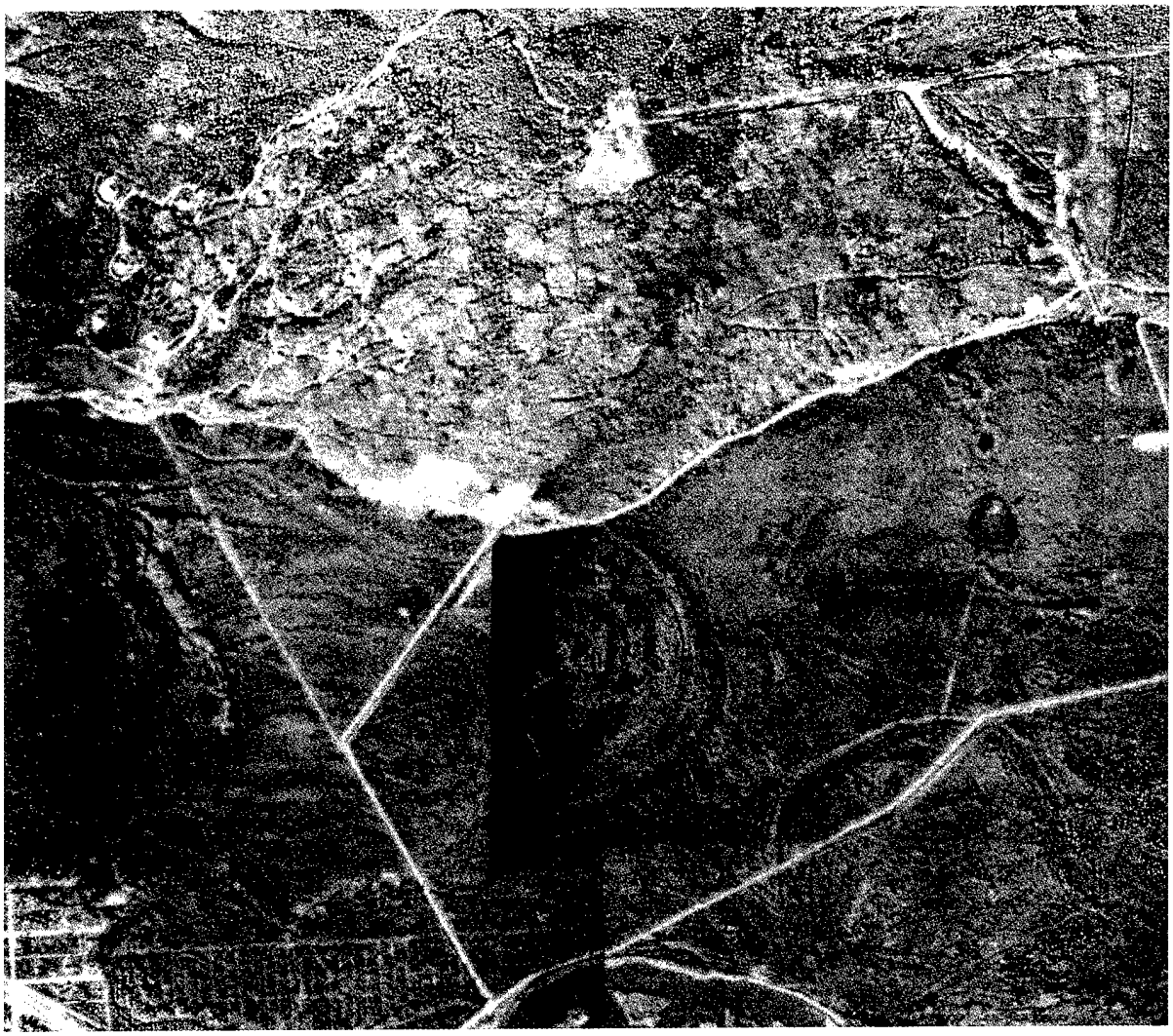

Figure 4. Aerial photograph mosaic of the region generally north of the Chena River from 9 September 1949. The approximate area of the Truck Fill Stand is outlined.

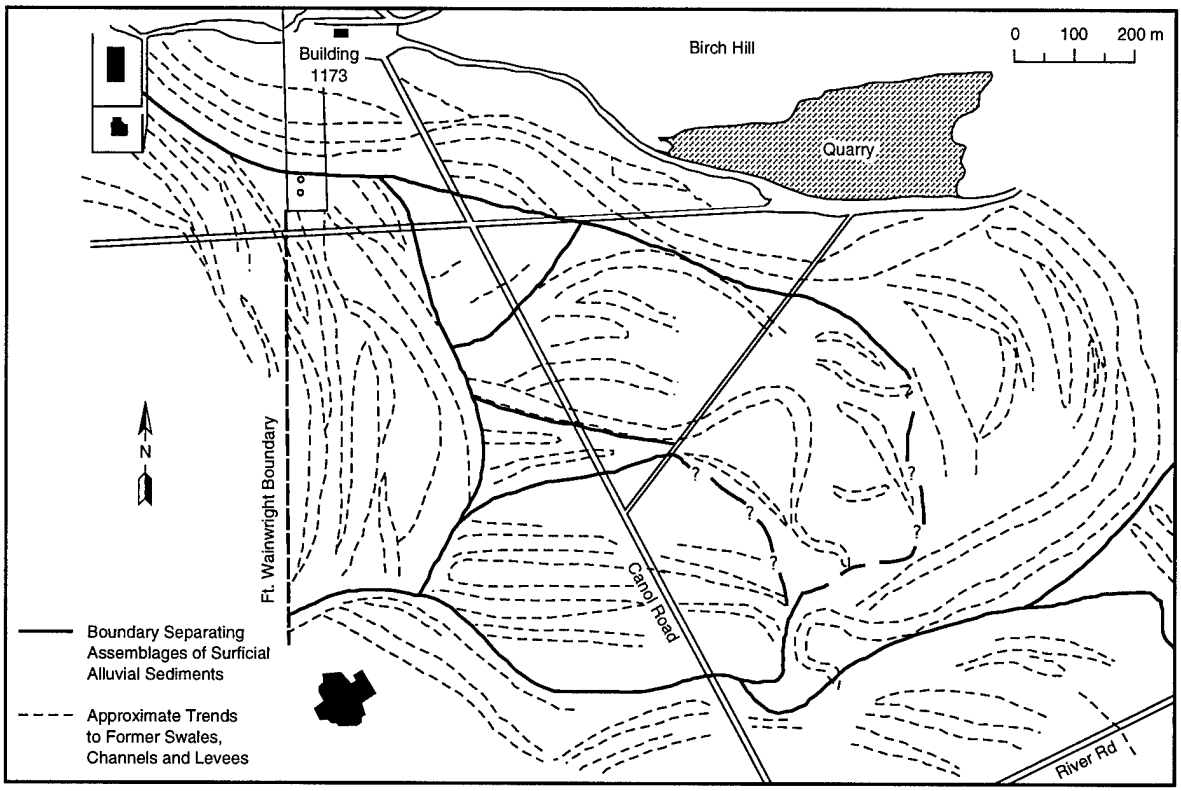

Figure 5. Assemblages of alluvial deposits distinguished by the trends of the point bars, swales, former channels, and levees north of the Chena River. Cross-cutting relationships of these features indicate the relative ages of the surficial deposits.

(Fig. 1 and 3). The Tank Farm is located on the south–southwest slope of Birch Hill where permafrost is probably absent owing to its southern exposure. Drilling shows that the Tank Farm area is generally blanketed by accumulations of eolian silt (loess). This silt overlies a 1- to 3-m-thick zone of moderately to highly weathered schist, which grades into unweathered schistose bedrock at depth. The Truck Fill Stand lies south of the Tank Farm in an area of alluvial deposits.

Arcuate patterns or meander scrolls on 1949 aerial photographs confirm the alluvial origins of the sediments, and cross-cutting relationships provide evidence on relative ages of different deposits (Fig. 4). The most prominent features within the site reflect a meandering channel migrating towards the northeast, with the youngest deposits existing in the outer-most loop, which encircles most of the site. Paleocurrents were presumably in a counter-clockwise direction around this loop. Cross-cutting the earliest deposits of this sequence, however, are the north–south trending swales near the western post boundary, indicating possibly secondary channel cut-offs or sloughs. The youngest sediments within this area, however, are those bordering River Road (Fig. 5) and within the Test Grid area. As is discussed in a later section, there is no clear relationship between the ages of sediments and the extent of permafrost development, which further complicates predictions of locations and extents of frozen zones. Prominent sloughs, however, tend to be zones of partial or complete thaw and may therefore be significant pathways of groundwater flow.

Canol Road and the adjacent pipeline extend southeast towards the Chena River within a cleared right-of-way (Fig. 1). There is significant thaw beneath the road and pipeline, with the top of permafrost generally at depths of 7 to 13 m (Lawson et al. 1993). The pipeline crosses the river at the railroad bridge and terminates at the Rail Off-Load Facility (ROLF), an area of point bar and swale deposits within a convex, northward loop in the Chena River (Fig. 1). More detailed descriptions of each site and historical accounts of contaminant sources are given by Ecology and Environment (1994).

METHODS OF INVESTIGATION

We have used several methods to develop an understanding of permafrost distribution, ground water distribution and movement, and the area's hydrogeology. These data are coupled to in-situ, site-specific measurements of ground water flow direction and velocity in monitoring wells.

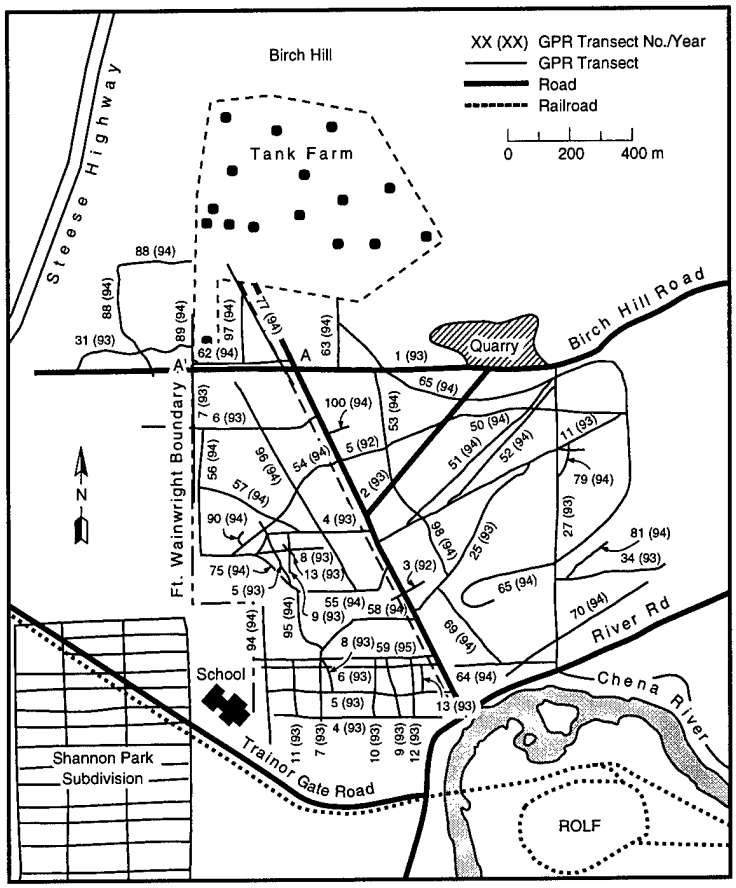

Figure 6. GPR transects in the OU-3 area north of the Chena River. Cross section A–A' is illustrated in Figure 11.

Ground-penetrating radar (GPR)

Ground-penetrating radar profiles were made along transects established on existing trails in the Canol Road area, some of which were cleared of recent vegetation by hydro-ax. Their locations were subsequently surveyed (Fig. 6). We profiled each transect by dragging antennas along the ground behind a tracked vehicle at a constant velocity of about 1 m/s. The antennas were situated approximately 6–7 m behind the vehicle. Event markers were placed artificially on the records at 10-m intervals. Scan durations, which are related to depth, were set to encompass the features of interest. Generally, we used 600 to 1200 ns for profiles with both 50- and 100-MHz antennas. The 1200-ns range penetrates approximately 40 m through frozen ground, yielding data from the bottom surface of permafrost. Scan durations of up to 2000 ns were used with the 50-MHz antennas in areas with much deeper (60-m) permafrost.

The radar system consisted of a Geophysical Survey Systems, Inc., SIR Model 4800 control unit, assorted antennas, cables, a GSSI DT6000 digital tape recorder, and a power supply. Appendix A gives a more complete description of GPR methods and theory.

Boreholes

We identified subsurface material types and permafrost horizons by drilling boreholes in 1993 and 1994. Drill sites (Fig. 7) were chosen according to the GPR data and preliminary interpretations of the site's geomorphic features based upon ground observations and aerial photography. Geologic logs provided data necessary to quantify GPR records, which provide vertical depths in terms of times of signal returns in nanoseconds, rather than true depths. Borehole and GPR records were subsequently combined to develop interpretive cross sections of permafrost and aquifer distribution. Piezometric surface measurements were also obtained from suprapermafrost, subpermafrost and unfrozen zone aquifers encountered by the drilling. Geologic logging of each borehole followed standard procedures.

Monitoring wells

Monitoring wells, generally in clusters of three at depths of about 10, 20 and 30 m, were drilled, logged and developed for use with a ground water flow system (see following section). Each monitoring well cluster is located within thawed, permafrost-free zones. Additional wells were drilled to below permafrost into the subpermafrost aquifer and pressurized to prevent their closure by ice growth (Fig. 8). Data from GPR surveys, borehole logs and geomorphic features, and other geological data were used to select monitoring well locations and provide representative ground water flow data.

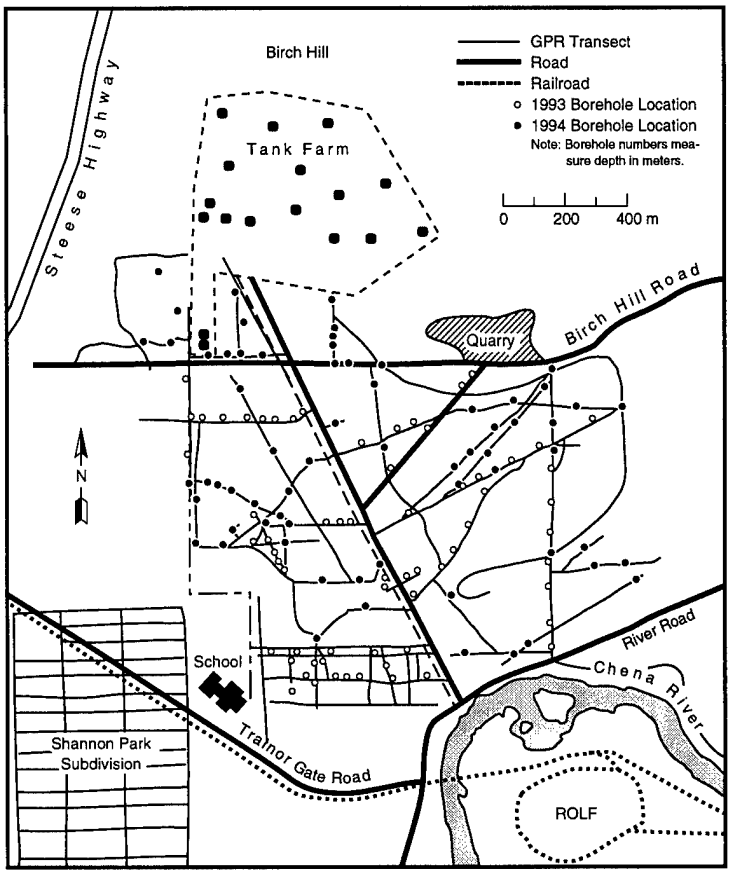

Figure 7. Ground-truth boreholes located on GPR transects.

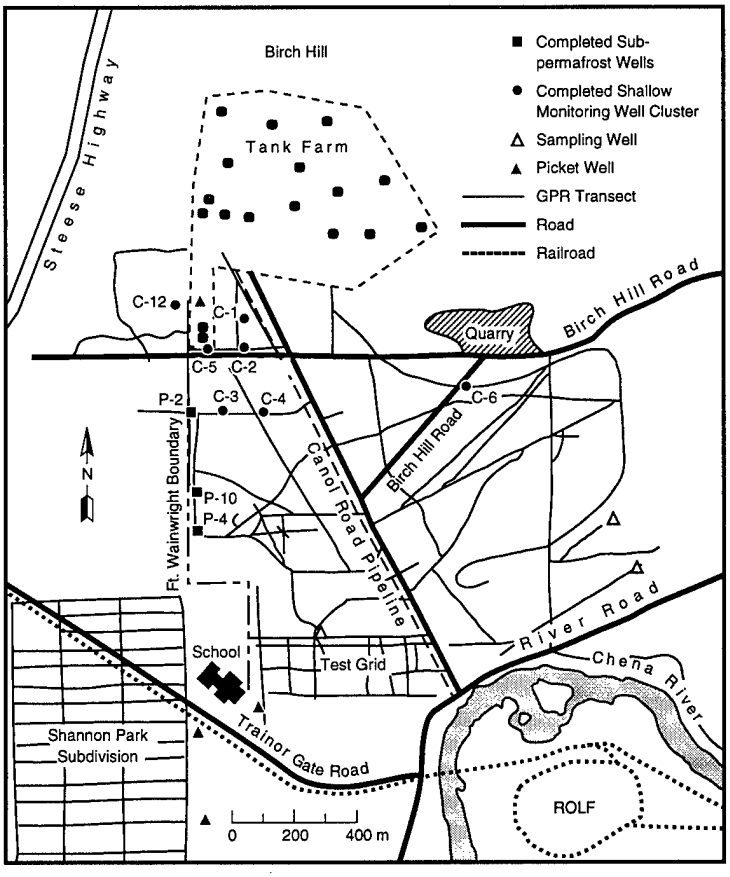

Figure 8. Current locations of monitoring wells with CRREL prototype flow systems installed.

Monitoring wells above and below the permafrost were installed and developed following standard procedures. Each monitoring well was drilled to a specified depth, at which a 3-m length of well screen was installed. All monitoring wells have a well screen, evaluated by laboratory testing at CRREL, that minimizes the restrictions to water movement, keeps finer sediment from infiltrating the well, and permits in-situ measurements with a prototype ground water flow system (Fig. 9). The well screen is ~2-in. (5 cm) i.d., continuous wire wrap, stainless steel with 0.060-in. (15-mm)

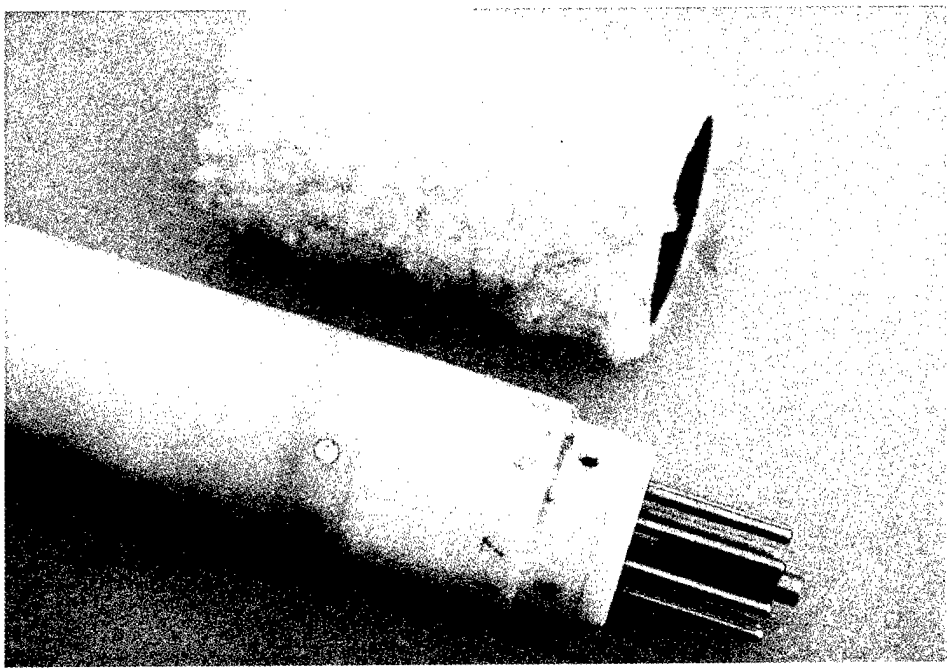

a. CRREL-modified flow sensor.

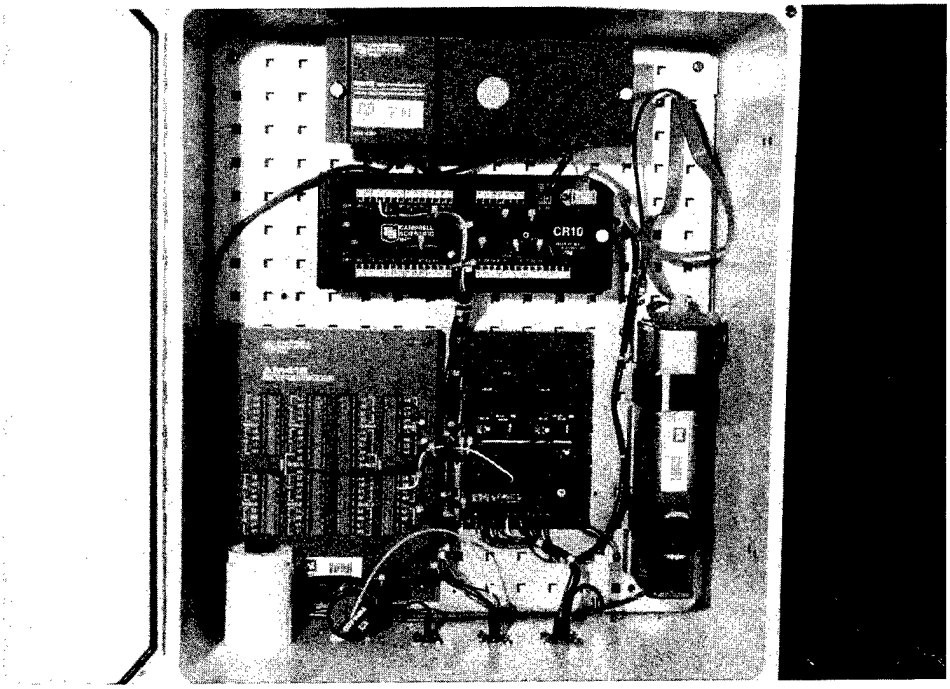

b. Electronic circuitry and data logger of the flow system.

Figure 9. Ground water flow monitoring system.

slot size. A filter sock with a mesh of 120- to 150-μm covers the outside of the screen (Fig. 9). After we installed the wells, each hole was allowed to collapse around the screen as a way to maintain minimally disturbed conditions. Monitoring wells drilled through permafrost were screened at a depth beginning 3 m below the bottom of the permafrost. During drilling through permafrost, we followed standard procedures to stop ground water from the suprapermafrost aquifer from flowing down into the hole.

Automated ground water flow system

CRREL's prototype ground water flow system uses the thermal tag and trace technique (e.g., Chapman and Robinson 1962, Hess 1982) to measure flow direction and seepage velocity in the monitoring wells in the Canol Road area (Fig. 8). This system employs a sensor that closely follows the configuration of a commercial probe, which had limited applicability to permafrost areas. Extensive work has developed a more refined system for accurately measuring the direction and magnitude of slowly flowing ground water (Williams et al. 1995).

The prototype system uses a sensor with four pairs of platinum Resistive Temperature Devices (RTDs) in steel tynes that are arrayed in a circular pattern around a point source heater (Fig. 9a). Heat is transferred preferentially by ground water flow from the heater to the RTD's. Conductive heat transfer occurs through glass beads in which the RTD tynes are imbedded.

Temperature fluctuations between paired RTDs relative to background levels are recorded. This temperature differential is then used to calculate the direction of flow and seepage velocity. Each sensor should be calibrated in a flume filled with materials representative of those surrounding each particular well screen to obtain absolute velocity measurements. A constant displacement pump is used to regulate seepage rates from 1 to 10 ft/day (0.3 to 3 m/day).

Flow sensors are suspended from steel rods lowered and locked into position in each well after orientation to magnetic north. The suspension system was designed at CRREL to ensure minimum slack in connections and precise orientation of the sensor at depth (Williams et al. 1995). The direction and velocity of seepage are measured hourly, with system functions controlled by a Campbell CR10XT data logger. Signals are transmitted and received through a CRREL-designed circuit board (Fig. 9b). In addition, a pressure transducer (Druck PDCR-35D) is also installed in each well and hourly fluctuations in the water level (piezometric surface) are recorded. Data stored within the logger are subsequently downloaded into a portable computer for analysis and graphical display.

As mentioned, flow sensors are calibrated within a flume. For this study it was filled with a commercially available sand mixture (sieve no. 8–12) that is generally representative of materials in each well screen interval. This calibration provides an empirical relationship between the sensor readings and seepage velocity, as well as direction. A more precise and accurate velocity measurement can be obtained by calibrating each sensor to the actual materials surrounding each well screen. The calibration used in this study produces a relative velocity that is considered accurate to within ±0.6 ft/day (±0.15 m/day).

ANALYSIS AND INTERPRETATION

We have developed preliminary maps of the permafrost distribution and hydrogeology of the Canol Road area that are based upon interpretation of the GPR records, borehole logs, terrain analyses and related data (e.g., Lawson et al. 1993, Ecology and Environment 1994) on the surficial geology and ground water conditions.

Permafrost distribution

Permanently frozen and unfrozen sediments in the Canol Road area are complexly distributed, with highly variable annual depths of thaw and depths to the bottom of permafrost. The spatial distribution of deep and shallow unfrozen zones, including the active layer above permafrost, are depicted in Figure 10a, while a second map (Fig. 10b) portrays the occurrence of unfrozen sediments beneath permafrost. Both maps show the locations of zones that are completely unfrozen but surrounded by permafrost.

Deep thaw zones—typically less than 3 to over 15 m deep—are commonly associated with disturbed terrain (e.g., roads and clearings), while shallower active layers of less than 3-m depth characterize undisturbed permafrost terrain (Fig. 10a). Areas with thin active layers (1.0 m or less) are commonly associated with thick permafrost that extends into bedrock. Areas or zones that are unfrozen from the surface to bedrock are com-

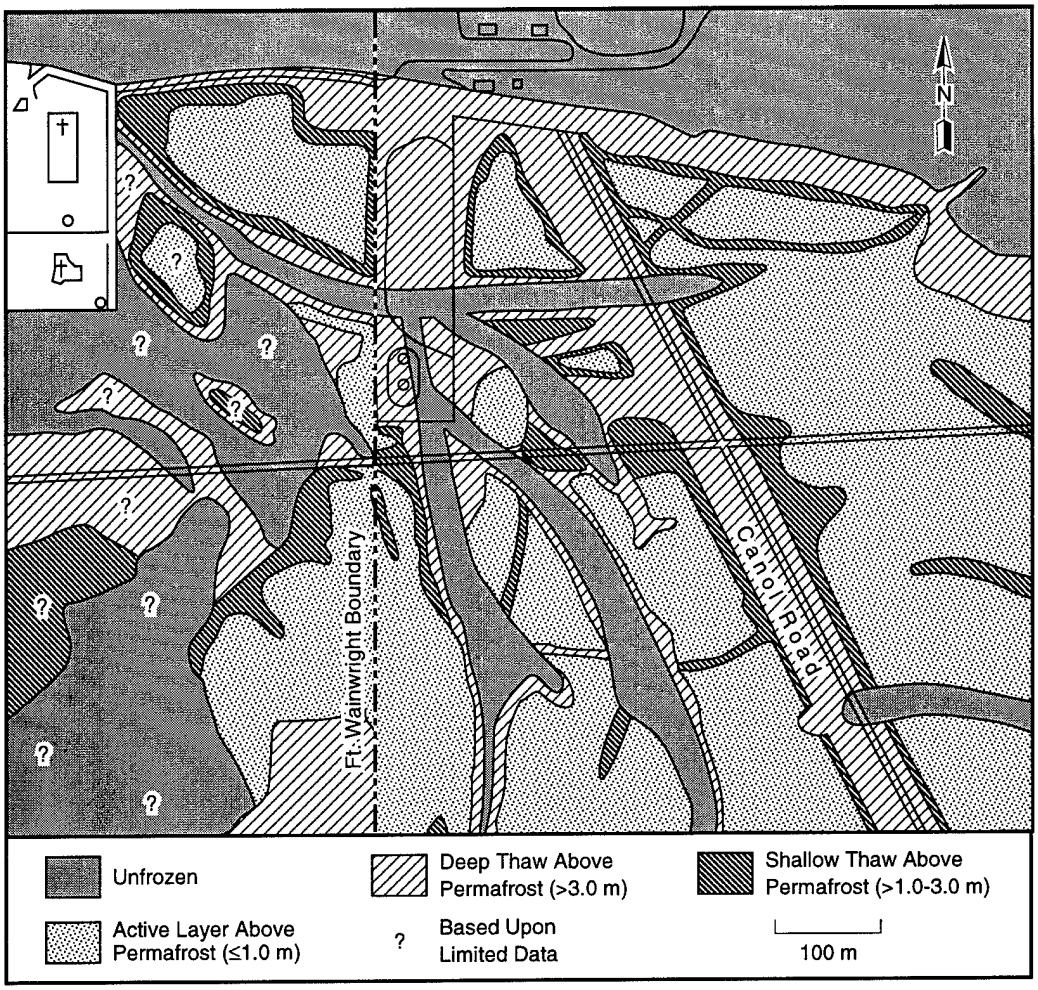

a. Characteristic depths of thaw and the locations of zones that are unfrozen from the surface into bedrock. Small, shallow drainageways and gullies are not identified on this map. These areas may locally exceed thaw depths by two or three times the cited depths. Completely thawed areas have peripheral shallow and deep thaw zones, which, unless quite wide, are omitted from the map to reduce clutter.

Figure 10. Preliminary maps of the Canol Road area. Maps made from unrectified aerial photographs taken on 20 May 1993. Interpretations are based upon GPR and borehole data and ground observations.

mon within former channels, swales or sloughs, resulting in an arcuate pattern that reflects the past alluvial activity in this area (Fig. 10). Thaw depths adjacent to such unfrozen areas are deeper, but often become shallow rapidly with distance away from them (Fig. 11).

Vegetation can tell us the approximate range of thaw depth in some areas. Stunted black spruce, for example, are usually growing on an active layer that is less than 1 m thick. Larger, healthy spruce, sometimes mixed with birch, may grow within areas having deeper annual thaw zones. Unfrozen areas of former sloughs and swales are commonly vegetated by large birch and aspen or poplar.

Permafrost extends from about 7 m depth near the base of Birch Hill to over 35 m south of the Truck Fill Stand and west of Canol Road (Fig. 12). Permafrost generally thickens, and depths to its base increase, with distance south of Birch Hill. Where unfrozen materials occur above bedrock, we presume that the bedrock is unfrozen at depth as well. The depth to bedrock ranges from several meters to over 40 m in the same area (see Fig. 13).

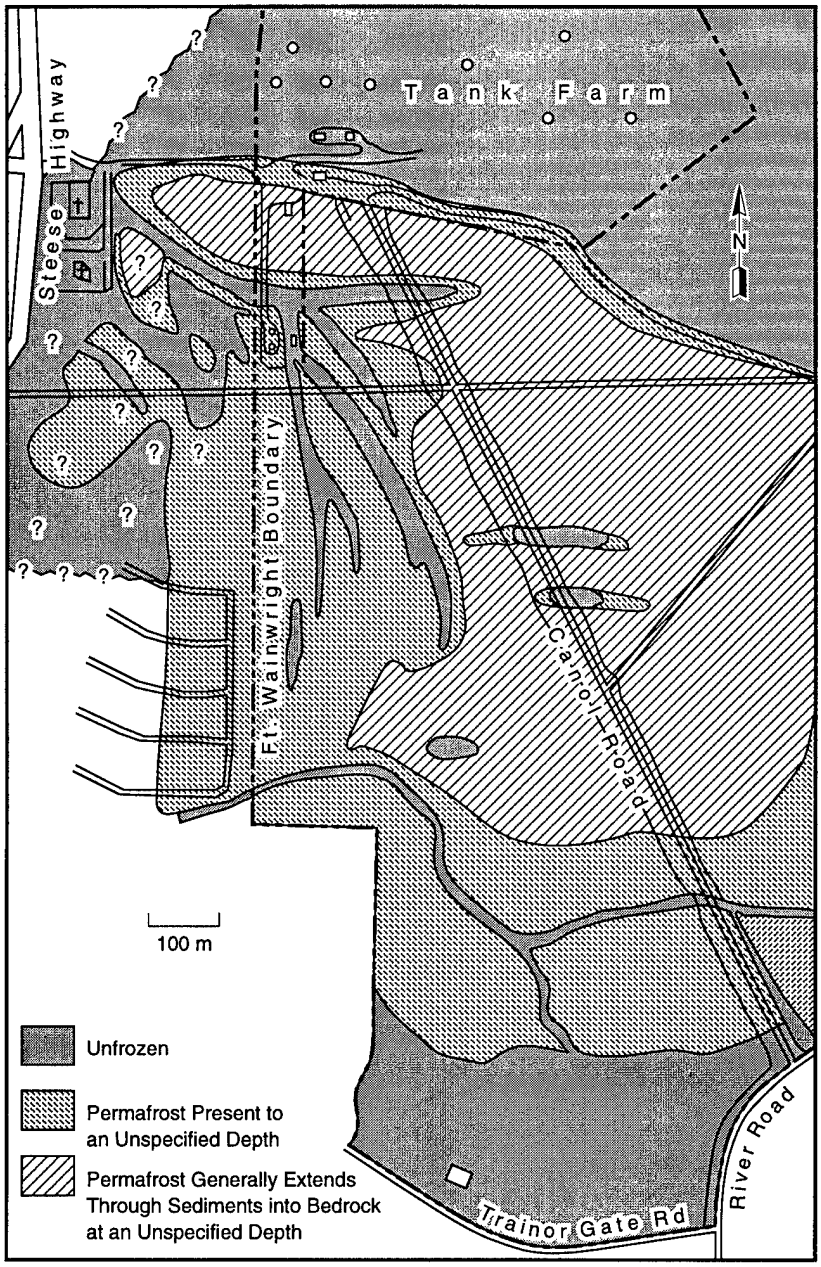

b. Presence or absence of unfrozen materials below the permafrost. Aquifers are usually present within the unfrozen materials. In the first unfrozen classification, the following applies—sediments thawed to bedrock; water bearing; bedrock presumed thawed. In the second classification, the following applies—sediments thawed between permafrost and bedrock; subpermafrost aquifer present. In the third classification, the following applies—water not encountered during drilling through weathered bedrock surface; locally sporadic and discontinuous thaw zones may be present at the sediment/bedrock interface, especially near thaw zones and adjacent to subpermafrost aquifer.

Figure 10 (cont'd).

Thus, there are large areas where sediments are perennially frozen an unknown depth into the underlying bedrock (Fig. 10b). Such areas laterally confine unfrozen and deeply thawed areas from one another, thereby affecting ground water flow. In other locations, permafrost thickness is less than the depth to bedrock; underlying sediments are unfrozen, as is the bedrock beneath them, and they generally contain ground water.

A particularly extensive area where bedrock is relatively shallow and sediments are frozen into it lies south and east of the Tank Farm (Fig. 10b). Because of its lateral extent, this area forms a nearly impenetrable barrier to deeper ground water migration from the east and south of the Truck Fill Stand, where there is a subpermafrost aquifer in unfrozen materials beneath the permafrost.

The data on bedrock depth indicate the existence of a buried valley trending northeast to southwest across the site in an area of discontinuous permafrost (Fig. 13). Because much of the Truck Fill Stand area is characterized by unfrozen sediments beneath permafrost, the bedrock valley appears to provide a connection for ground water in

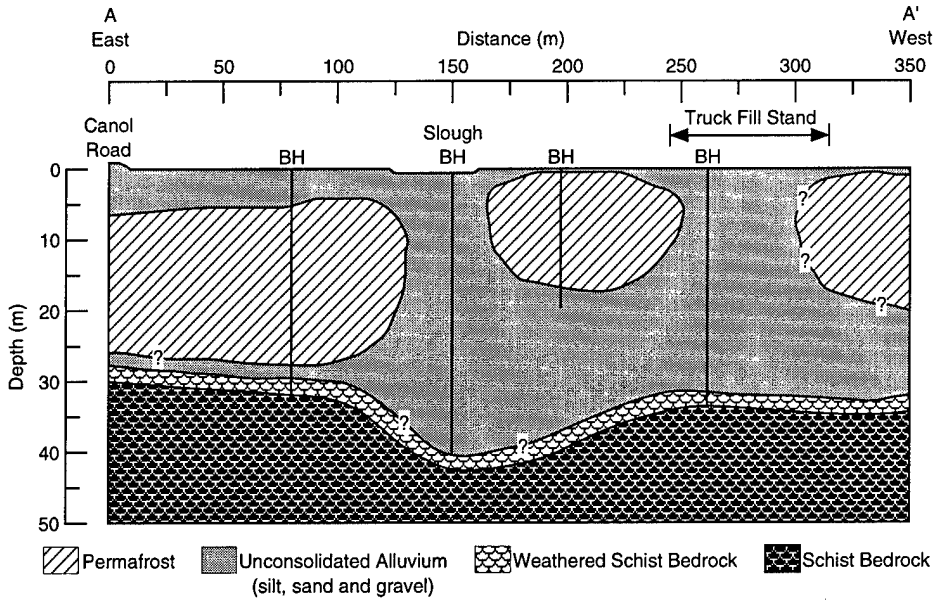

Figure 11. Cross section A-A' (survey line 62 (94), Fig. 6) illustrating the relationship between areas of permafrost that extend into bedrock and the rapid transition from unfrozen to frozen materials.

Birch Hill with the subpermafrost aquifer south of the site.

In addition, the trend and location of the buried valley align reasonably well with a gully present on the hillside within the Tank Farm (Fig. 10b). We speculate that this ravine and the buried valley are related, and that both follow a fracture zone within the bedrock. This fracture zone may also be sufficiently permeable to transmit ground water within the bedrock.

Aquifers

Unfrozen sediments of former channels in the Canol Road area represent aquifers through which there may be significant flow of ground water (Fig. 10a). These aquifers evidently merge near the Truck Fill Stand and are continuous, with more extensive unfrozen zones near the Steese Highway. They are also probably continuous with the subpermafrost aquifer south and west of the site (Fig. 10b). Unfrozen colluvial sediments at the base of Birch Hill may also represent a significant shallow aquifer, providing a route for ground water migration parallel to the top of the slope.

Deeply thawed areas beneath Canol Road and the Truck Fill Stand support a suprapermafrost aquifer. Unfrozen channel deposits provide a direct connection between this suprapermafrost aquifer and the subpermafrost aquifer.

The large area of permafrost frozen to bedrock with a thin active layer east and southeast of the site (Fig. 10a and b) limits the potential interaction of both supra- and subpermafrost aquifers in the study area with the aquifer further to the east. It will thereby also affect the hydraulic gradient within the site and may result in directions of flow that respond to more local ground water sources. Birch Hill may influence ground water flow, given its elevation and the potential effects of water influx at its surface. Exposures of schist within quarries on the south side of Birch Hill reveal numerous fractures from which water commonly seeps. Such fractures may therefore be zones of highly localized ground water flow within Birch Hill and beneath the Chena River flood plain, creating localized piezometric gradients in the suprapermafrost and subpermafrost aquifers that are difficult to predict.

The subpermafrost aquifer, however, will also be in communication with ground water further south in the Chena River area (Fig. 10b). This area is more likely to be controlled by the subregional flow system, which numerous studies have shown to have a general west to northwest gradient (e.g., Williams 1970, Péwé et al. 1976, Ecology and Environment 1994). Therefore, both local and subregional ground water controls may determine flow patterns and velocities within the subpermafrost aquifer of the immediate site. Flow within the unfrozen channel aquifers may be affected because of their communication with the subpermafrost aquifer.

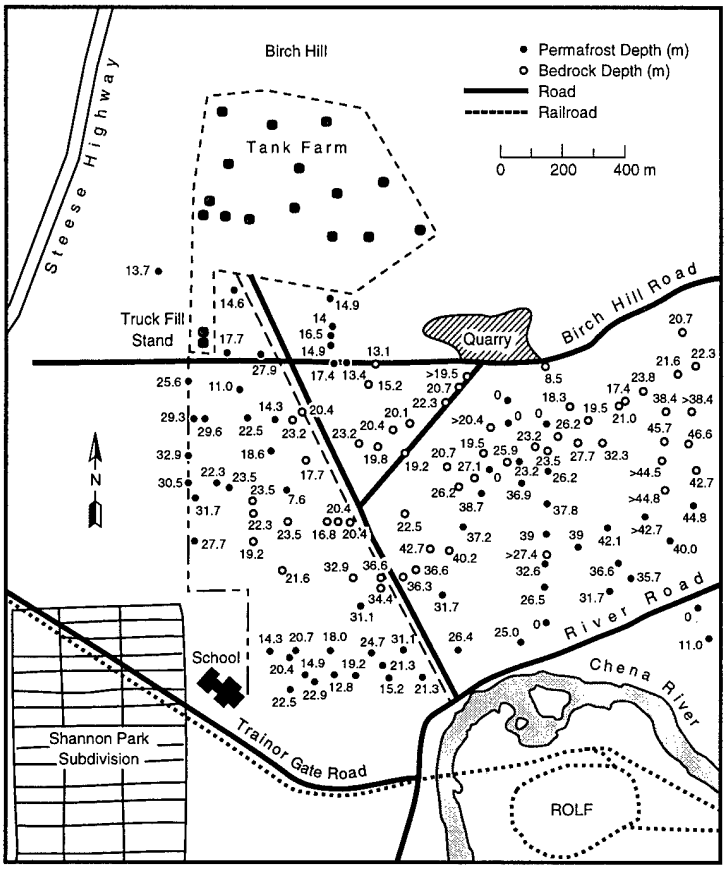

Figure 12. Depths to the bottom of permafrost from boreholes in the Canol Road area.

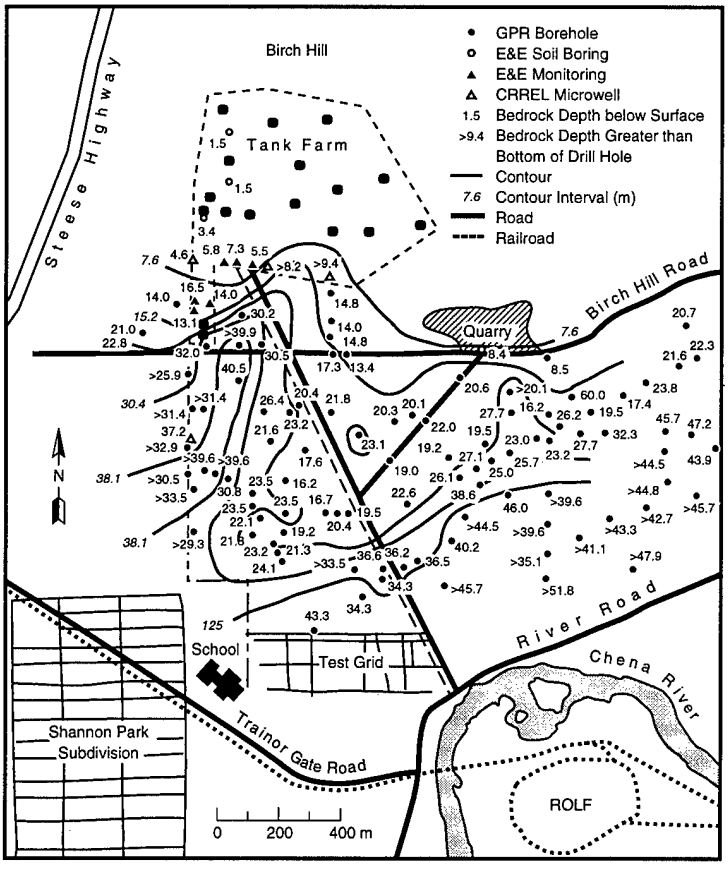

Figure 13. Preliminary map of the depth to bedrock from borehole data in the Canol Road area; contour interval is 1.5 m.

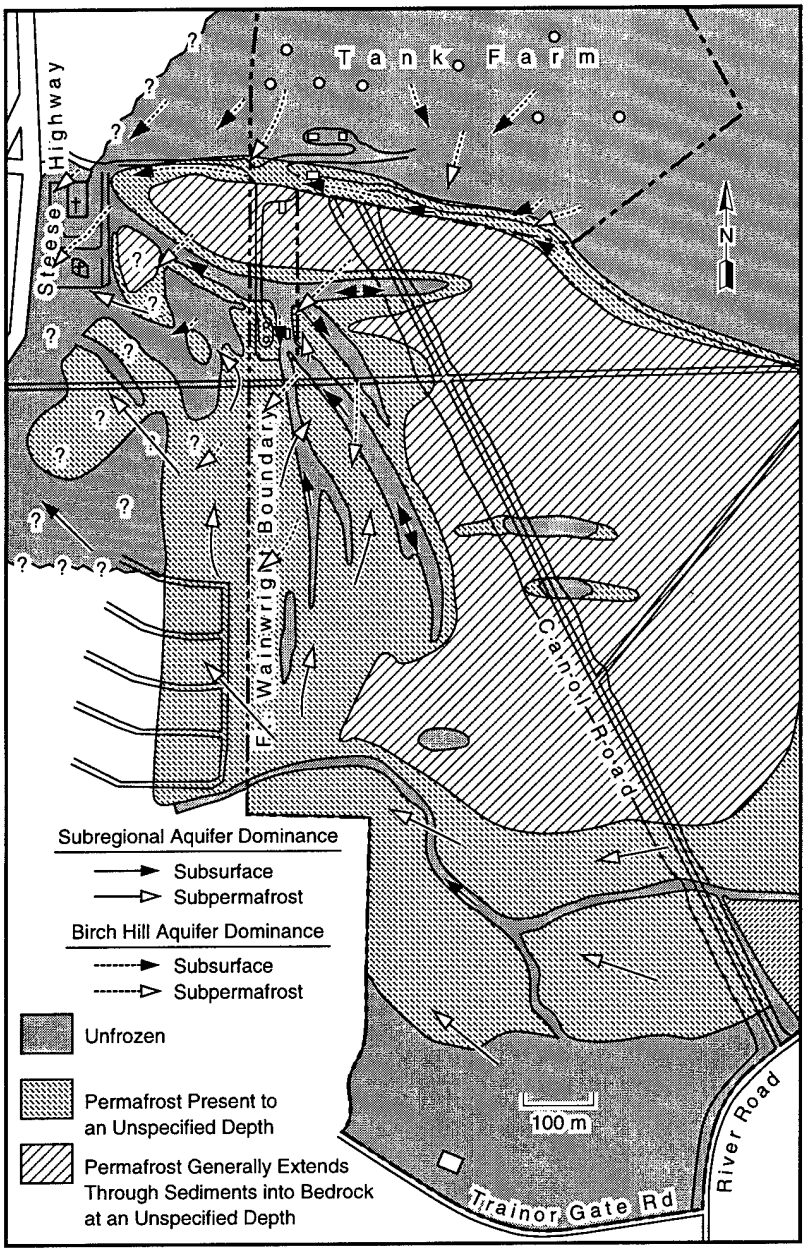

Figure 14. Potential near-surface flow paths depicted for two scenarios: a hydraulic gradient dominated by the subregional aquifer and a more local system dominated by Birch Hill. The resultant direction and velocity of flow for each scenario differ significantly in both the subpermafrost aquifer and in unfrozen zones linked to it. Map made from unrectified aerial photographs taken on 20 May 1993. Interpretations are based upon GPR and borehole data and ground observations.

GROUND WATER FLOW PATTERNS

The movement of ground water in the Canol Road area will reflect the confining and bounding conditions imposed by the permafrost and bedrock. Permafrost constraints on ground water flow include 1) the extensive area east and southwest of the site where permafrost extends into the bedrock, 2) the zone of permafrost that is frozen to bedrock within the upper half of the Truck Fill Stand area, 3) the relatively limited occurrence and configuration of unfrozen zones above bedrock, 4) the shallow depth of annual thaw over areas immediately adjacent to the Tank Farm, Truck Fill Stand and Canol Road pipeline, and 5) the depth and thickness of the subpermafrost aquifer peripheral to the site (Fig. 10a and b). Surface and near-surface flows are also influenced by the topography, including such factors as the steep ravine and slope of Birch Hill, the morphology of former swales and channels that cross the area, and active layer thickness, which will affect the volume and rate of surface runoff (Fig. 10a).

We considered two scenarios of the Canol Road area hydrogeology to be possible. The first assumes that localized aquifers within Birch Hill and local climatic events (e.g., precipitation, spring runoff) are the predominant water sources determining ground water flow patterns and rates. The second assumes that the subregional aquifer associated with the Chena River is the most important control on site-specific flow patterns. As will be discussed briefly later, the interaction of both systems probably determines ground water conditions north of the Chena River.

Potential pathways for near-surface ground water movement and the possible connections into unfrozen zones, and thus the subpermafrost aquifer, are shown relative to the shallow characteristic depths of thaw on Figure 14. The near-surface ground water system is located above permafrost where the thaw zone is

sufficiently thick to permit a continuous to mostly continuous aquifer. Thin active layers of 1.0 m or less are unlikely to support a continuous ground water aquifer, although sporadic, isolated ones may exist in topographic lows. Thus, water may move through a suprapermafrost aquifer within the Truck Fill Stand area, the suprapermafrost thaw bulb below Canol Road, and the narrow unfrozen zone above bedrock along the base of Birch Hill in the Tank Farm area (Fig. 15). The flow direction responds to a gradient generated mainly by local conditions, including seepage through the near-surface materials and weathered bedrock of Birch Hill, and by runoff associated with precipitation or snowmelt.

The near-surface, perched ground water communicates with the subpermafrost aquifer through the unfrozen zones of the former channel deposits (Fig. 14). Once within these unfrozen zones, local gradients, hydraulic conductivities and sedimentary–stratigraphic properties determine seepage direction and velocity. The impermeable nature of the permafrost confines the aquifers within these deposits, possibly directing lateral movements (Fig. 16). Areas with a downward gradient will result in movement into the subpermafrost aquifer.

The subpermafrost aquifer may respond to hydraulic gradients produced by either the subregional aquifer within the Chena and Tanana riv-

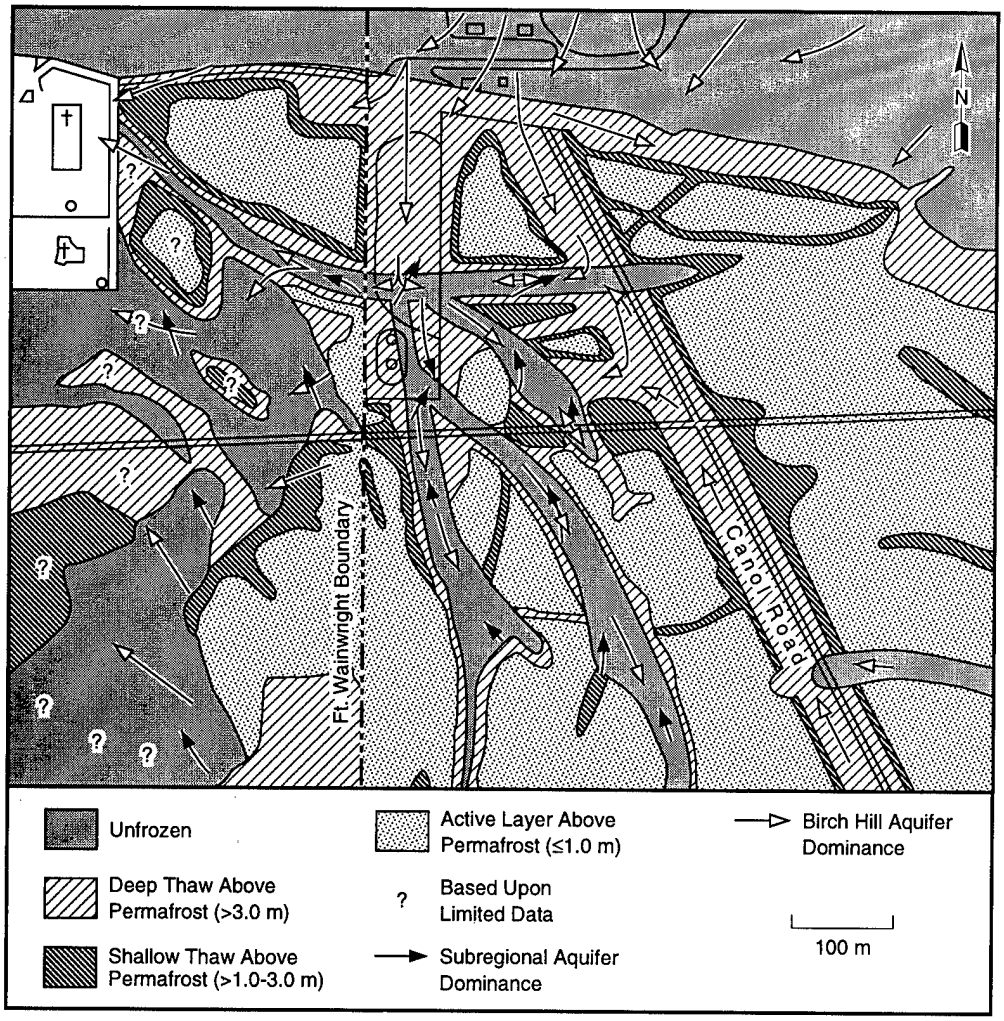

Figure 15. Potential deep aquifer flow paths depicted for two scenarios: a hydraulic gradient dominated by the subregional aquifer and a more local system dominated by Birch Hill. The resultant direction and velocity of flow for each scenario differ significantly in both the subpermafrost aquifer and in unfrozen zones linked to it. Map made from unrectified aerial photographs taken on 20 May 1993. Interpretations are based upon GPR and borehole data and ground observations.

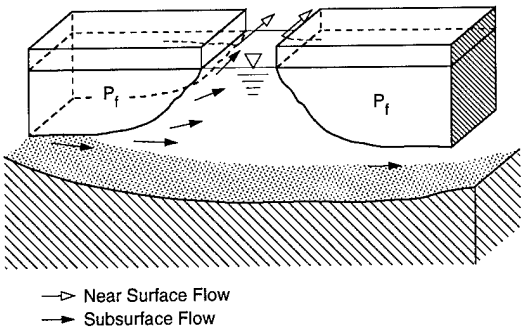

Figure 16. Potential interaction and flow directions between a subpermafrost aquifer and an unfrozen zone, such as a former swale or channel.

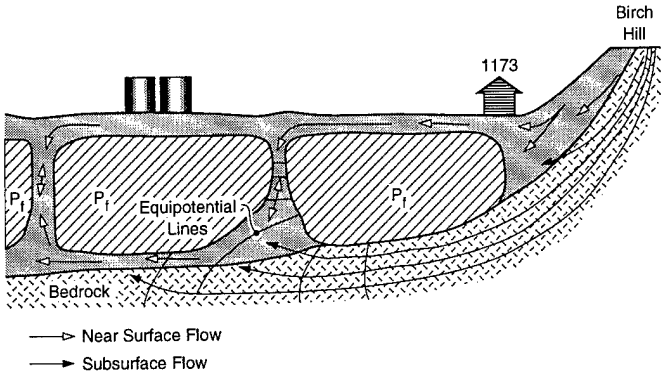

Figure 17. Idealized subpermafrost and suprapermafrost flow patterns associated with an aquifer within the bedrock in Birch Hill. Flow below the permafrost responds to the hydraulic gradient of Birch Hill. Flow that trends E–W is the result of permafrost confinement in unfrozen former channels.

ers' alluvium or a bedrock aquifer associated with Birch Hill (Fig. 15). In either case, the constraints of permafrost are relevant. Barriers caused by permafrost extending into bedrock will affect flow patterns for both scenarios, resulting in mainly a north–south trend, the actual direction responding to the local gradient. A system dominated by flow from water within the bedrock in or below Birch Hill (referred to hereafter as the localized aquifer within Birch Hill) would result in subsurface flow that generally parallels the direction of slope, resulting in upward directed flow after passing beneath permanently frozen materials (Fig. 17). Also relevant to this scenario are the down-gradient water table fluctuations that respond to stage fluctuations in the Chena River, thus affecting the ultimate baseline and hydraulic gradient between the Canol Road OU-3 sites and the Chena River in the downtown Fairbanks area.

We consider it probable that both the subregional Chena and Tanana river system aquifer and the localized aquifer within Birch Hill significantly affect ground water flow directions and seepage velocities in the Tank Farm and Truck Fill Stand area. Moreover, the dominance of one system over the other may vary seasonally in response to changes in runoff and infiltration of snowmelt or rain. We expect seasonal periods of little to no flow within the unfrozen channel deposits, as well as in deep thaw zones above the permafrost.

In addition, the effects of the subregional aquifer on subpermafrost flow may vary seasonally, in some cases raising water levels within the Canol Road area and perhaps inducing reversals in flow direction. Changes will be most pronounced within the unfrozen channel deposits that are surrounded by permafrost, and include both east–west and north–south trending features. Subregionally controlled directions will be mostly northward in the north–south unfrozen zones south of the Truck Fill Stand, while mostly north–northeast in the subpermafrost aquifer (Fig. 14). We anticipate southerly flow in these unfrozen zones and southwesterly in the subpermafrost aquifer if the localized aquifer within Birch Hill controls the local hydraulic gradient. This scenario of interacting aquifers in determining flow patterns is consistent with deep (30 m) flow measurements made during the early winter period of 1994–95.

SEEPAGE MEASUREMENTS

Limited measurements of ground water flow with the CRREL prototype system suggest that patterns within the study area for the early to mid-winter period of October 1994 to January 1995 mainly respond to locally generated hydraulic gradients interacting with the impermeable permafrost (Table 1).

During early to mid-winter, water levels were slowly falling while seepage directions and velocities remained relatively constant to slowly falling (Table 1). Seepage velocities, based upon the calibration to a no. 8–12 sand mixture, typically ranged from 0.5 to 1 m/day, with maximum values of 1.7 to 2.6 m/day measured in two 10-m-deep wells (Table 1). These isolated higher values may reflect localized controls on water movement, or perhaps inaccuracies for a particular well at-

Table 1. Relative seepage velocity and direction data in monitoring wells.

Well number	Well depth (ft) (m)	October				November				December				January				October–January averages	
		Avg dir (°)	Std dev (°)	Avg vel (ft/day) (m/day)	Std dev (ft/day) (m/day)	Avg dir (°)	Std dev (°)	Avg vel (ft/day) (m/day)	Std dev (ft/day) (m/day)	Avg dir (°)	Std dev (°)	Avg vel (ft/day) (m/day)	Std dev (ft/day) (m/day)	Avg dir (°)	Std dev (°)	Avg vel (ft/day) (m/day)	Std dev (ft/day) (m/day)	Dir (°)	Vel (ft/day) (m/day)
MWC-1	100.3 (30.6)	167.65	5	1.51 (0.46)	0.1(0.03)	162.00	8	1.50 (0.46)	0.10 (0.03)	113.00	23	2.00 (0.61)	0.8 (0.24)	120.00	3	3.60 (1.10)	0.2 (0.06)	140.66	2.15 (0.65)
MWC-1A	60.0 (18.3)	82.38	2	2.08 (0.63)	0.1 (0.03)	82.00	2	2.10 (0.64)	0.10 (0.03)	85.00	2	2.10 (0.64)	0.1 (0.03)	86.00	2	2.20 (0.67)	0.1 (0.03)	83.85	2.12 (0.64)
MWC-1B	30.0 (9.1)																		
MWC-2	90.5 (27.6)	215.03	5	1.56 (0.48)	0.1 (0.03)	217.00	4	1.50 (0.46)	0.10 (0.03)	201.00	9	1.70 (0.52)	0.5 (0.15)	198.00	3	2.50 (0.76)	0.1 (0.03)	207.76	1.81 (0.55)
MWC-2A	60.0 (18.3)	127.11	2	2.55 (0.78)	0.1 (0.03)	125.00	2	2.50 (0.76)	0.10 (0.03)	120.00	3	2.50 (0.76)	0.1 (0.03)	122.00	3	2.30 (0.70)	0.1 (0.03)	123.53	2.46 (0.75)
MWC-2B	30.0 (9.1)	216.83	2	3.44 (1.05)	0.1 (0.03)														
MWC-3	90.0 (27.4)	240.30	3	1.59 (0.49)	0	245.00	3	1.60 (0.49)	0.10 (0.03)	245.00	2	1.50 (0.46)	0.1 (0.03)	245.00	4	1.50 (0.46)	0.1 (0.03)	243.83	1.55 (0.47)
MWC-3A*	60.0 (18.3)	124.18	2	4.78 (1.46)	0.2 (0.06)	131.00	6	5.50 (1.68)	0.70 (0.21)	144.00	2	7.50 (2.29)	0.4 (0.12)	149.00	1	7.90 (2.41)	0.2 (0.06)	137.04	6.42 (1.96)
MWC-3B	30.5 (9.3)	37.37	2	2.29 (0.70)	0.1 (0.03)														
MWC-4	85.5 (26.1)	200.26	9	3.00 (0.91)	0.2 (0.06)	195.00	14	2.80 (0.85)	0.20 (0.06)	213.00	18	2.60 (0.79)	0.2 (0.06)	217.00	2	2.40 (0.73)	0.1 (0.03)	206.31	2.70 (0.82)
MWC-4A	60.5 (18.4)	156.33	7	2.91 (0.89)	0.2 (0.06)	157.91	1	2.90 (0.88)	0.10 (0.03)	157.00	2	2.90 (0.88)	0.1 (0.03)	156.00	1	3.00 (0.91)	0.1 (0.03)	156.81	2.93 (0.89)
MWC-4B	30.5 (9.3)	39.00	4	1.87 (0.57)	0.1 (0.03)														
MWC-5	90.5 (27.6)	206.36	10	1.11 (0.34)	0.1 (0.03)	179.00	28	1.50 (0.46)	0.50 (0.15)	140.00	3	2.10 (0.64)	0.1 (0.03)	158.00	11	2.30 (0.70)	0.1 (0.03)	170.84	1.75 (0.53)
MWC-5A	60.5 (18.4)	161.62	2	2.98 (0.91)	0.2 (0.06)	162.56	1	2.95 (0.90)	0.10 (0.03)	163.00	2	3.00 (0.91)	0.2 (0.06)					162.39	2.97 (0.91)
MWC-5B	29.5 (9.0)	320.59	5	7.64 (2.33)	0.3 (0.09)	305.00	1	8.00 (2.44)	0.10 (0.03)	308.00	1	8.10 (2.47)	0.1 (0.03)						
MWC-6	30.0 (9.1)	44.86	6	1.36 (0.42)	0.1 (0.03)														
MWC-7	90.0 (27.4)					200.00	3	2.50 (0.76)	0.30 (0.09)	200.00	3	2.70 (0.82)	0.2 (0.06)	195.00	3	2.70 (0.82)	0.2 (0.06)	198.33	2.63 (0.80)
MWC-7A	60.0 (18.3)	81.87	2	4.10 (1.25)	0.1 (0.03)	80.00	1	4.10 (1.25)	0.10 (0.03)	79.00	1	4.20 (1.28)	0.1 (0.03)	78.00	2	4.20 (1.28)	0.1 (0.03)	60.97	4.15 (1.27)
MWC-7B	30.0 (9.1)	174.93	14	1.88 (0.57)	0.8 (0.24)														
MWC-8	59.5 (18.1)	269.71	146	1.06 (0.32)	0.1 (0.03)	335.00	8	1.10 (0.34)	0.10 (0.03)	339.00	16	1.10 (0.34)	0.1 (0.03)	299.00	7	1.30 (0.40)	0.1 (0.03)	310.68	1.14 (0.35)
MWC-8A	29.5 (9.0)																		
MWC-9	59.5 (18.1)																		
MWC-9A	29.5 (9.0)																		
MWC-11	119.0 (36.3)																		
MWC-11A	89.0 (27.1)																		
MWC-11B	59.2 (18.0)					111.22	11.55	1.61 (0.49)	1.58 (0.48)	113.95	7.43	1.42 (0.43)	0.12 (0.04)	100.00	38	0.90 (0.27)	0.2 (0.06)	108.39	1.31 (0.40)
MWC-11C	29.5 (9.0)																		
MWC-12	29.5 (9.0)					114.23	3.92	1.93 (0.59)	0.17 (0.05)	113.00	8.00	1.50 (0.46)	0.20 (0.06)	132.00	14	1.30 (0.40)	0.1 (0.03)	119.74	1.58 (0.48)

*Velocities reflect electronic failure and not true velocity increase.

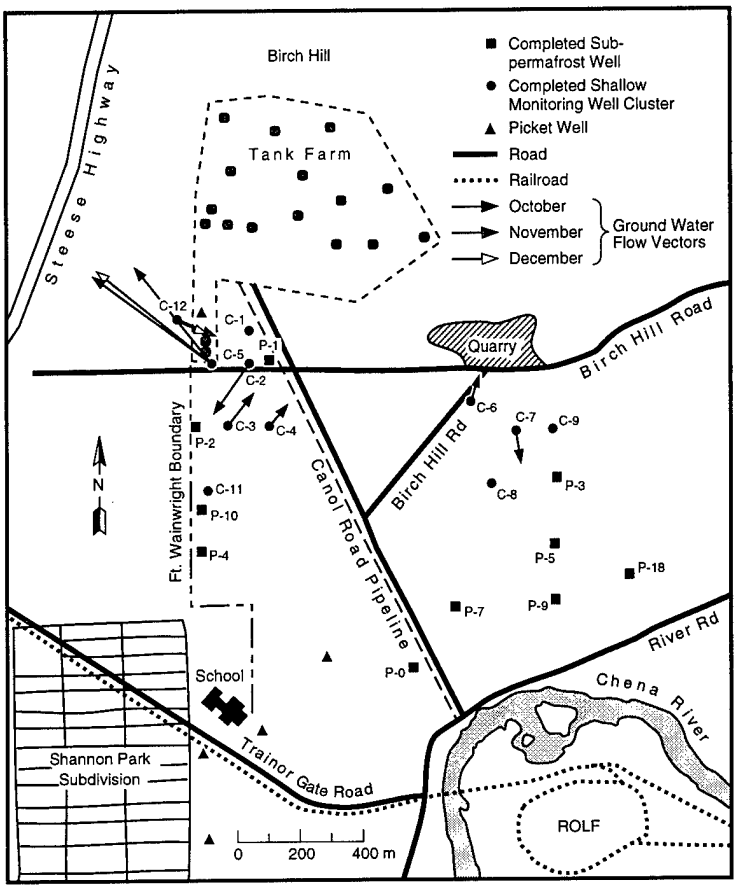

a. 10-m wells.

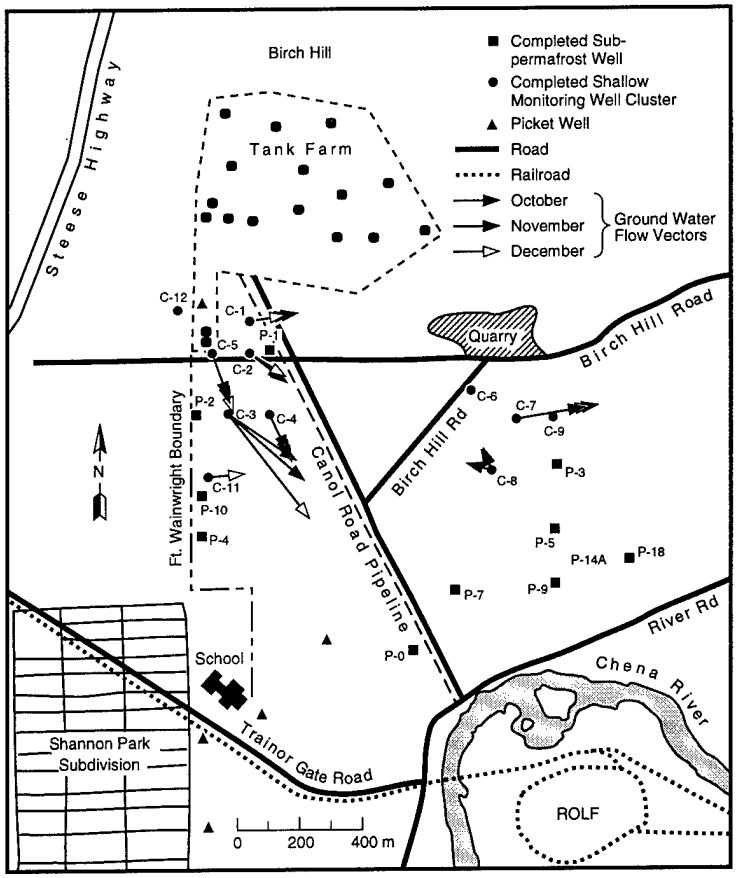

b. 20-m wells.

Figure 18. Monthly mean flow vectors calculated from daily flow system measurements during the October 1994 to March 1995.

c. 30-m wells.

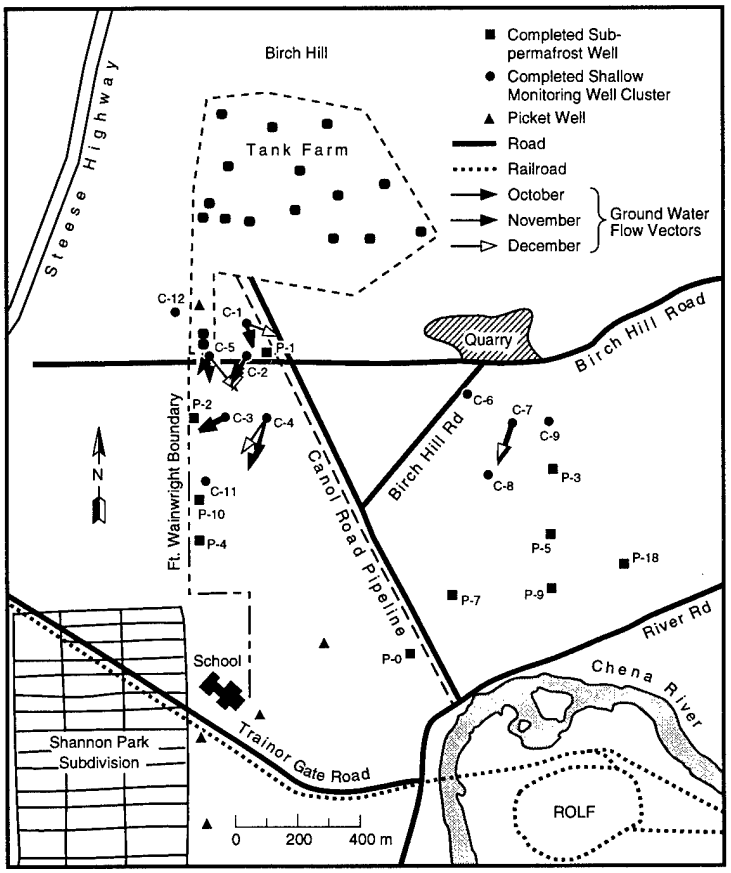

Figure 18 (cont'd).

tributable to the current probe calibration in a standard no. 8–12 sand mixture.

The 30-m-deep wells have fairly consistent seepage velocities and directions of flow, while the 20-m-deep wells exhibit slightly greater variability in direction from month to month (Fig. 18). Velocities remain fairly constant but at a rate greater than those of the 30-m depth. The 20-m well data exhibit a mostly south–southeast flow pattern within thaw zones that trend mainly northwest to southeast (Fig. 18b). Eastern trending directions of flow (e.g., MWC-1, MWC-12) are consistent with well locations within thaw zones that trend mainly east to west (Fig. 15 and 18c).

Data from the 30-m-depth monitoring wells exhibit a south to southwest pattern with velocities ranging from about 0.5 to 1 m/day (Fig. 18c and 19c). These data vary little from month to month. Their consistency in direction and rate probably reflects their location at or below the base of the permafrost.

The patterns exhibited by the 10-m wells are of much greater variability (Table 1) than those at either 20 or 30 m (Fig. 18c and 19c). This variability is apparently a function of the confining effect of permafrost. Certain wells, notably MWC-12, had a reversal in flow direction within this period.

The flow data from early to mid-winter indicate that seepage directions and velocities vary with well depth, this variability apparently reflecting the proximity and geometry of the permafrost. Surrounding and confining permafrost, which extends from about 25 to 35 m below the surface, locally controls flow directions, while interaction with the subpermafrost aquifer of the area may induce highly variable horizontal and vertical gradients and seepage rates. Directions of flow may therefore deviate greatly from the subregional pattern of flow (e.g., MWC-12, MWC-1, Table 1). The variability in the 10- and 20-m well data are consistent with their location within thaw zones bounded by permafrost. In contrast, the more consistent flow pattern of the 30-m-depth wells probably reflects the overall flow pattern of the deeper aquifer in this area because measurements are close to the bottom of the permafrost. These data also indicate that the hydraulic gradient is controlled locally by an aquifer within or north of Birch Hill.

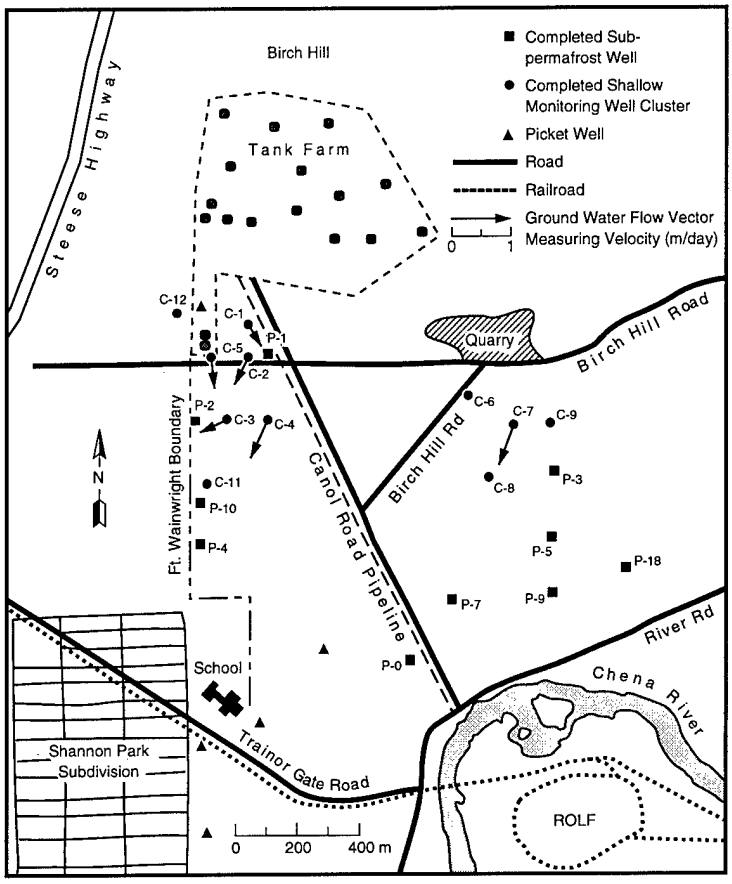

a. 10-m wells.

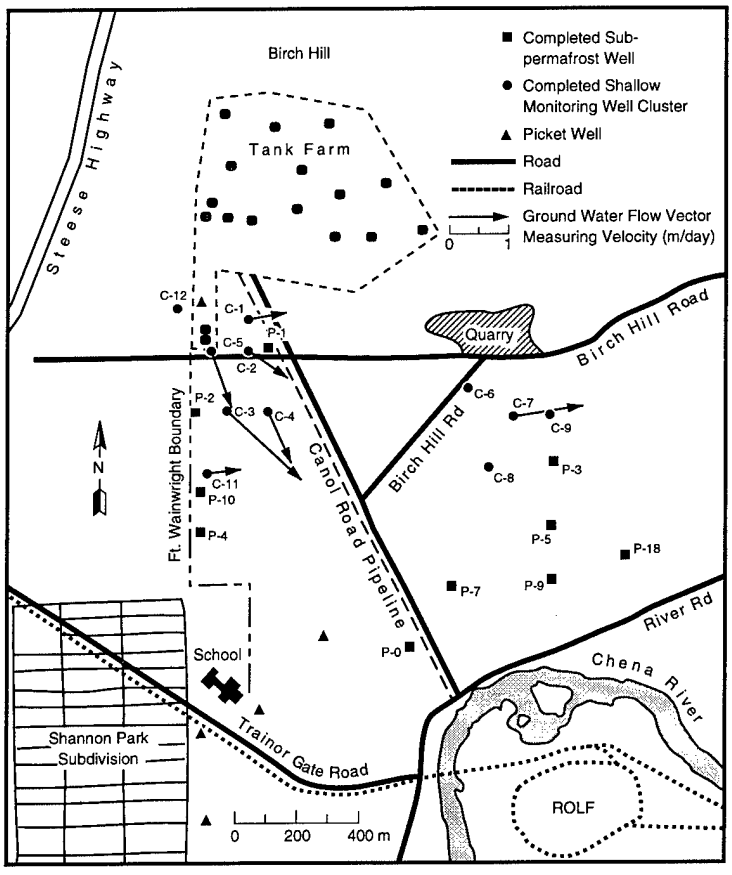

b. 20-m wells.

Figure 19. Mean flow directions for October 1994 to March 1995.

CONCLUSIONS

Hydrogeological conditions are extremely complex within the Canol Road area because of the complex distribution of aquifers within the discontinuous permafrost. Aquifers occur within the unfrozen materials above (suprapermafrost), below (subpermafrost) and within (intrapermafrost) the impermeable, permanently frozen alluvial sediments. Zones that are completely unfrozen from the surface into the bedrock interconnect the supra- and subpermafrost aquifers. Near-surface flow generally takes place in suprapermafrost aquifers within deeply thawed, disturbed areas, where the top of permafrost lies at depths ranging from a few meters to over 15 m, as well as within unfrozen former swales or channels. In addition, areas where materials are deeply frozen and possess only thin active layers interrupt the continuity of the subpermafrost aquifer, as well as confine or isolate suprapermafrost aquifers from unfrozen zones. In particular, a zone to the east and southeast of the site severely limits communication of ground water with the aquifer further south near the Chena River.

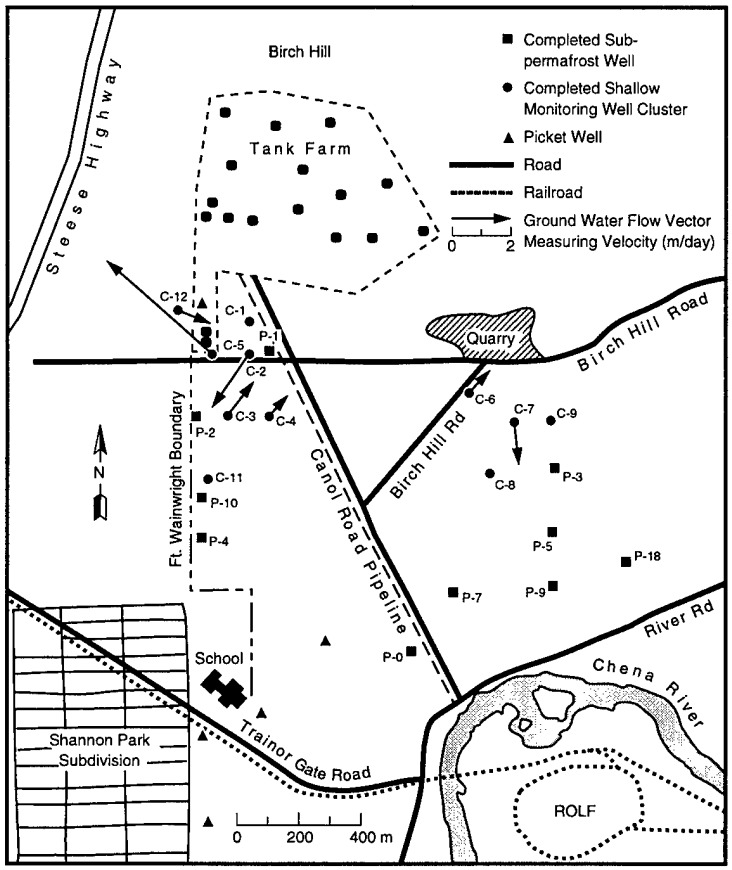

c. 30-m wells.

Figure 19 (cont'd).

Seepage measurements with flow sensors in monitoring wells for the period of October 1994 to January 1995 indicate that flow directions at the 30-m depth were consistently to the south–southwest. At the 10- and 20-m depths, flow is much more variable in orientation and velocity. This variability reflects the effects of permafrost and its configuration. Seepage data suggest that the local gradient is responding to a hydraulic gradient north of the site, including Birch Hill.

These limited data suggest that ground water movement within the Canol Road area is mainly controlled by local water sources and hydraulic gradients. The overall directions of flow are therefore not the same as the subregional pattern of westerly to northwesterly flow. Rather, they trend mainly south to southwest in the subpermafrost aquifer. Directions may vary greatly from site to site within unfrozen zones surrounded by permafrost. Northeast–southwest trending zones tend to have a southwesterly flow, while east–west trending zones show mainly easterly flow directions.

These results are critical to predicting ground water movement and the fate and transport of contaminants. Simple water table elevation measurements from wells across the area that are commonly taken quarterly or monthly at some sites cannot be used to develop a hydraulic gradient and predict site-specific flow patterns.

Site-specific flow patterns often differ significantly from the general subregional flow pattern. Therefore, measurements that consider the effects of permafrost provide accurate data on ground water movement and site specific movements and should be used to analyze contaminant fate or migration.

Potential pathways for contaminant migration include 1) unfrozen former channels trending both east–west and north–south across the site, 2) the subpermafrost aquifer above bedrock where it is interconnected with the unfrozen zones and the unfrozen southern slope of Birch Hill, and 3) near-surface, suprapermafrost aquifers within disturbed areas of Canol Road, Lazelle Road, Birch Hill Road, the Tank Farm and the Truck Fill Stand. Our initial data suggest that the migration of con-

taminants is controlled locally and varies seasonally, including reversals in transport direction.

Although we cannot yet predict the directions and rates of ground water movement within the Canol Road area with certainty, continued analyses of the distribution of frozen and unfrozen materials that are coupled to flow measurements in monitoring wells, including new subpermafrost wells, will allow us to develop a much clearer picture of the overall patterns above, within and below the permafrost. Moreover, long-term data acquisition will reveal whether flow parameters change seasonally or annually, and will give us insight into the dominant aquifer controlling the ground water system of the Canol Road area.

RECOMMENDATIONS

Ground water flow patterns require further analysis to define potential contaminant migration pathways in the discontinuous permafrost within the Tank Farm, Truck Fill Stand and Canol Road areas. Preliminary data are insufficient to model ground water flow accurately, particularly the role of local (Birch Hill) or subregional aquifers in ground water movement. Monitoring wells should be installed in Birch Hill to define the local hydraulic gradients. Water quality parameters should also be analyzed for wells at various depths in each aquifer within and external to the study area to further define water sources affecting site-specific ground water flow. Year-round flow system measurements are required to identify seasonal variability in direction and seepage velocity.

LITERATURE CITED

Chapman, H.T. and A.E. Robinson (1962) A thermal flowmeter for measuring velocity of flow in a well. U.S. Geological Survey Water Supply Paper, 544-E.

Ecology and Environment (1994) Remedial investigations report, Operable Unit 3, Fort Wainwright, Alaska, Volumes 1, 2, and 3. Prepared for the U.S. Army Engineer District, Alaska.

Hess, A.E. (1982) A heat pulse flowmeter for measuring low velocities in boreholes. U.S. Geological Survey Open File Report, 82-699.

Hopkins, D.M., T.N.V. Karlstrom and others (1955) Permafrost and ground water in Alaska. U.S. Geological Survey Professional Paper 264-F.

King, P.B. (1969) Tectonic map of North America (1:5,000,000). U.S. Geological Survey Map.

Lawson, D.E., S.A. Arcone, J.C. Strasser, A. Delaney, C. Williams and D. Albert (1993) Geological and geophysical analyses of permafrost and ground water conditions, Fort Wainwright, Alaska. Progress Report prepared for the U.S. Army 6th ID and U.S. Army Engineer District, Alaska.

Péwé, T.L. (1958) Geologic map of the Fairbanks D-2 Quadrangle, Alaska. U.S. Geological Survey Geology Quadrangle Map GQ-110.

Péwé, T.L., J.W. Bell, R.B Forbes and F.R. Weber (1976) Geologic map of the Fairbanks D-2 SE Quadrangle, Alaska. U.S. Geological Survey Miscellaneous Investigations Series Map I-942.

Shannon and Wilson, Inc. (1992) Potential offsite ground water contaminant migration, west boundary, Fort Wainwright, Alaska. Prepared for the U.S. Army Engineer District, Alaska.

Williams, J.R. (1970) Ground water in the permafrost regions of Alaska. U.S. Geological Survey Professional Paper, 696.

Williams, C.R., J.S. Morse, D.E. Lawson, D.E. Garfield, J.D. Strasser and T. Tantillo (1995) An automated monitoring system for site-specific, in situ ground water flow analyses, Fort Wainwright, Alaska. Interim Draft Report for U.S. Army Alaska, Directorate of Public Works, and U.S. Army Engineer District, Alaska.

APPENDIX A: GROUND-PENETRATING RADAR OPERATION AND THEORY

General operation

A Geophysical Survey Systems, Inc., SIR Model 4800 radar control unit, assorted antennas, cables, a GSSI DT6000 digital tape recorder, and a power supply were used in this study. The control unit keys the transmitter on and off at 50 kHz (synchronized with the receiver), sets the scan rate (rate at which echo scans are compiled, generally 25.6 scans/s), scan time range and the time range gain to be applied to the scans. The transmit antenna radiates a broadband pulse that lasts from only a few to tens of nanoseconds (ns). A separate, identical receive antenna is employed because echoes can return from near-surface targets before the transmit antenna has stopped radiating. The received signals are converted by sampling into an audio frequency facsimile for filtering, amplification and recording.

Field procedures

Transects were established along trails in the Canol Road area and profiled by dragging the antennas along the ground, about 6–7 m behind a tracked vehicle. All surveys were done with the antennas polarized perpendicular to the transect direction so that the more intense, but unorthodox, H-plane pattern was in the line of the transect.

Event markers were placed artificially on the records at measured intervals, generally every 10 m. Scan durations were set to encompass the features of interest, which always occurred within the depth of the noise floor visible on the oscilloscope incorporated in the control unit. Generally, we used 500 to 1000 ns for profiles with both the 50- and 100-MHz antennas as the deeper sections of water beneath permafrost usually occurred between 400 and 600 ns into the records. Scan durations up to 2000 ns for the 50-MHz antennas were used in areas with much deeper (to 60 m) permafrost.

Data recording and processing

All data were recorded at a scan rate of 25.6/s, and a scan sampling density of 512 or 1024 eight-bit words. The slow dragging speed resulted in a recorded scan about every 4 cm. All data were stacked five-fold, which marginally affected detail as the stacked horizontal data density was about one scan per 20 cm. Data recorded when antenna movement was stalled were deleted from the total record. After editing, the lengths of the records between distance markers were equalized (i.e., "justified") to compensate for changes in towing speed. Later processing reduced background ringing (e.g., from surface meltwater), alleviated overall gain variations resulting from inconsistent antenna–ground coupling, and enhanced vertical resolution using deconvolution. Data were displayed as echo-time-of-return vs. profile distance using either wiggle trace or line intensity format. Individual scans are easily retrieved with the software.

Data interpretation is generally based on the simple echo delay formula

$$d = ct/2n \qquad \text{(A1)}$$

where d is the depth of a reflector in centimeters, t is the echo time delay in nanoseconds and c is the speed of electromagnetic waves in a vacuum (30 cm/ns). The quantity n is often replaced by $\varepsilon^{1/2}$, where ε is the dielectric constant (approximately 5.3–6 for frozen alluvium). The factor of 2 in eq A1 accounts for the round-trip propagation path of the pulse and applies only to reflections from horizontally flat interfaces extending several in-situ wavelengths, or to scattering from point sources. Equation A1 can be applied to several layers successively if n is known for each layer and the delay times to each layer interface are easily picked off the record. Measurements made during the summer, when conditions had remained dry for over 6 weeks, reveal that a round-trip propagation time of 100 ns corresponds to a depth of about 6.5 m in permafrost, and 24 ns corresponds to 1 m of surface thaw.

Proper translation of echo time of return into depth requires a complicated process known as migration. Successful migration requires detailed knowledge of the subsurface velocity structure. Our knowledge of permafrost and thaw velocity comes from correlations between GPR and borehole data, along with previous studies of refraction in the Canol area. Migration is not necessary when subsurface interfaces are fairly horizontal, as they are in this study. In viewing the GPR profiles it must be remembered that there is a very large compression in the horizontal direction.

Antennas and radiation

All antennas used are resistively loaded dipoles that radiate a pulse containing about 2 to

2.5 cycles. The 50-MHz surveys were performed with a pair of unshielded (metallic shielding mitigates back radiation) strings of resistors. The transmit and receive antennas were separated by 3.3 m to prevent overloading the receiver by the 800-W peak power transmitter. The transmitter keyed the receiver along a fiber optic cable to reduce cable noise.

The 100-MHz antennas were commercially obtained (Model 3207, GSSI, Inc.) flared dipoles with a tapered resistive loading. The antennas were backshielded and housed in separate units placed 2 m apart. The transmitter is rated at 800 W peak power. All waveforms had a 3-dB bandwidth of about 35%. The received pulse waveforms of the 100-MHz antennas were similar to those of the 50 MHz.

Theoretical transmit radiation patterns for point dipoles are nonuniform, with nulls and lobes in planes parallel (E-plane) and perpendicular (H-plane), respectively, to the antenna axis. These features occur in the angular directions $\psi = \pm\sin^{-1}(1/n)$ measured from vertical, where n is the real part of the refractive index of the propagation medium. For frozen alluvium with $n = 2.3$, $\psi = \pm 26°$.

The effective transmit–receive directivity patterns are for a horizontal, unshielded, finite-size radar antenna operating monostatically on the ground. The H-plane pattern is perpendicular to the antenna axis and, therefore, along our profile directions. This orientation helps to ensure that we were profiling the ground directly beneath us rather than to the sides. These patterns are not affected significantly by the finite separation of transmit and receive antennas, which is much less than the ground water depths investigated. The patterns are more directive than for a single transmit antenna owing to multiplication of the identical transmit and receive directivities. The patterns may be considered to be the response to an isotropic, polarization-insensitive, nondispersive point target.

REPORT DOCUMENTATION PAGE

Form Approved
OMB No. 0704-0188

1. AGENCY USE ONLY (Leave blank)	2. REPORT DATE	3. REPORT TYPE AND DATES COVERED
	May 1996	

4. TITLE AND SUBTITLE

Geological and Geophysical Investigations of the Hydrogeology of Fort Wainwright, Alaska: Part I. Canol Road Area.

5. FUNDING NUMBERS

6. AUTHORS

Daniel E. Lawson, Jeffrey C. Strasser, Jodie D. Strasser, Steven A. Arcone, Allan J. Delaney and Christopher Williams

7. PERFORMING ORGANIZATION NAME(S) AND ADDRESS(ES)

U.S. Army Cold Regions Research and Engineering Laboratory
72 Lyme Road
Hanover, New Hampshire 03755-1290

8. PERFORMING ORGANIZATION REPORT NUMBER

CRREL Report 96-4

9. SPONSORING/MONITORING AGENCY NAME(S) AND ADDRESS(ES)

U.S. Army Engineer District, Alaska
for the Environmental Department, Public Works
Directorate, U.S. Army Alaska
Fort Wainwright, Alaska

10. SPONSORING/MONITORING AGENCY REPORT NUMBER

11. SUPPLEMENTARY NOTES

12a. DISTRIBUTION/AVAILABILITY STATEMENT

Approved for public release; distribution is unlimited.

Available from NTIS, Springfield, Virginia 22161

12b. DISTRIBUTION CODE

13. ABSTRACT (*Maximum 200 words*)

The hydrogeology of Fort Wainwright, Alaska, is extremely complex because of the relatively impermeable discontinuity of permafrost, which controls the distribution and dimensions of the aquifer. Aquifers occur above, below and adjacent to permanently frozen materials, as well as within thaw zones surrounded by permafrost. This complexity makes it difficult to predict the direction and rate of ground water flow, as well as its seasonal and annual variability. Considerable problems exist in locating suspected contaminant plumes, identifying source areas, defining transport paths and evaluating contaminant fate. This report summarizes the results of ongoing investigations of the permafrost and ground water conditions within the northwestern part of the Fort Wainwright cantonment area, north of the Chena River. Data from ground-penetrating radar, drilling, ground water flow sensors, aerial photographs and ground observations were used to delineate aquifer distribution and develop a conceptual physical model of hydrogeological conditions. Ground water seepage velocity and direction, which were measured during early to mid-winter 1994–95, reflect the role of local water sources and permafrost distribution in determining ground water flow patterns. Other factors, including the vertical and lateral extent of permafrost, a bedrock aquifer, and the alluvial origins of unfrozen sediments and landforms, are apparently more important than the subregional aquifer in determining ground water conditions during winter. Contaminant migration will be strongly affected by these factors as well.

14. SUBJECT TERMS

Alluvium
Conceptual model
Ground penetrating radar
Ground water
Hydrogeology
Permafrost

15. NUMBER OF PAGES
32

16. PRICE CODE

17. SECURITY CLASSIFICATION OF REPORT	18. SECURITY CLASSIFICATION OF THIS PAGE	19. SECURITY CLASSIFICATION OF ABSTRACT	20. LIMITATION OF ABSTRACT
UNCLASSIFIED	UNCLASSIFIED	UNCLASSIFIED	UL